

# Spectrophotometry of 237 stars in 7 Open Clusters

Lori Clampitt

and

David Burstein

Department of Physics and Astronomy,

Arizona State University,

Tempe, AZ 85287-1504

Email: clampitt@accesscom.com; burstein@samuri.la.asu.edu

## ABSTRACT

Spectrophotometry is presented for 237 stars in 7 nearby open clusters: Hyades, Pleiades, Alpha Persei, Praesepe, Coma Berenices, IC 4665, and M39. The observations were taken by Lee McDonald and David Burstein using the Wampler single-channel scanner on the Crossley 0.9m telescope at Lick Observatory from July 1973 through December 1974. Sixteen bandpasses spanning the spectral range 3500Å to 7780Å were observed for each star, with

bandwidths 32Å, 48Å or 64Å. Data are standardized to the Hayes–Latham system to mutual accuracy of 0.016 mag per passband.

The accuracy of the spectrophotometry is assessed in three ways on a star-by-star basis. First, comparisons are made with previously published spectrophotometry for 19 stars observed in common. Second, (B–V) colors and *wby* colors are compared for 236 stars and 221 stars, respectively. Finally, comparisons are made for 200 main sequence stars to the spectral synthesis models of Kurucz, fixing  $\log g = 4.0$  and  $[\text{Fe}/\text{H}] = 0.0$ , and only varying effective temperature. The accuracy of tests using *wby* colors and the Kurucz models are shown to track each other closely, yielding an accuracy estimate ( $1\sigma$ ) of 0.01 mag for the 13 colors formed from bandpasses longward of the Balmer jump, and 0.02 mag for the 3 colors formed from the three bandpasses below the Balmer jump. In contrast, larger scatter is found relative to the previously published spectrophotometry of Bohm-Vitense & Johnson (16 stars in common) and Gunn & Stryker (3 stars).

We also show that the scatter in the fits of the spectrophotometric colors and the *wby* filter colors is a reasonable way to identify the observations of which specific stars are accurate to  $1\sigma$ ,  $2\sigma$ , ... As such, the residuals from both the filter color fits and the Kurucz model fits are tabulated for each star where it was possible to make a comparison, so users of these data can choose stars according to the accuracy of the data that is appropriate to their needs.

The very good agreement between the models and these data verifies the accuracy of these data, and also verifies the usefulness of the Kurucz models to define spectrophotometry for stars in this temperature range ( $>5000$  K). These data define accurate spectrophotometry of bright, open cluster stars that can be used as a secondary flux calibration for CCD-based spectrophotometric surveys.

*Subject headings:* open clusters; open cluster stars — spectrophotometry

## 1. Introduction

The existing spectrophotometry available in computer-accessible form (The Stellar Spectrophotometric Atlas, Gunn & Stryker 1983; hereafter SSA; The Catalog of Stellar Spectrophotometry, Adelman et al. 1989; hereafter CSS) tends to concentrate either on stars for stellar synthesis work, or stars of special interest (e.g., Ap stars; see Adelman et al.). Spectrophotometry of other stars also exists (e.g., Breger, 1976; Bohm-Vitense &

Johnson 1977 (hereafter BVJ); Ardeberg & Virefors 1980), but these data are not yet in computer-readable format. Even then, only the study of BVJ explicitly tried to sample stars in nearby open clusters. A bit earlier than the BVJ observations were taken, Lee McDonald and one of the authors (DB) decided to obtain spectrophotometric data for a set of open cluster stars. During 1973–4, 237 open cluster stars were observed using a scanning grating and a photomultiplier detector; an instrument no longer in general use. Any such observations today are likely obtained with CCD-based instrumentation.

Given the different detector systematics of photomultipliers and CCDs, and given the resurgence of interest in obtaining accurate fluxed data on stars and galaxies with CCDs, these kind of data are still of interest to many workers. Of the 237 stars in our survey, only 25 stars are in common with previous studies. However, 236 stars have BV colors and 221 have uvby colors to which we can quantitatively compare our results. In addition, spectrophotometry of such a large set of open cluster stars with a range of age but otherwise similar metallicity is a good test for the Kurucz (1992, 1993) stellar synthesis models.

The spectrophotometry for 237 stars, using 16 bandpasses from 3600–7800Å is presented in § 2. The seven open clusters observed are Hyades (Hya), Pleiades (Ple), Alpha Persei (Per), Praesepe (Pra), Coma Berenices (Com), IC 4665 (IC4), and M39. Comparisons to published spectrophotometry are also given in § 2. Comparisons to Johnson B–V and Strömngren  $u-v$ ,  $v-y$  and  $u-b$  colors are made in § 3. The comparison to the models of Kurucz is given in § 4. We show that these comparisons reasonably lead to a quantitative means of assessing the accuracy of spectrophotometry on a star-by-star basis in § 5. Our summary is given in § 6 and individual stars of special interest are discussed in Appendix A.

## 2. Observations, Calibrations and Data

### 2.1. Observations

The observations of these open cluster stars were taken by Lee McDonald and David Burstein during the period July 1973–Dec 1974, with the Wampler (1966) scanning spectrometer attached to the 0.9m Crossley telescope at Lick Observatory. Table 1 lists the clusters observed in order of increasing age. Parameters listed include Galactic latitude ( $b$ ) and longitude ( $l$ ), nominal distance and distances estimated here using a fiducial zero-age main sequence line ( $d$ ), the value of  $(E(B-V))$  used here, and estimated metallicity ( $[Fe/H]$ ). Table 2 gives the observing log, also noting the secondary standard star used for each night (see discussion below).

A one-channel ITT FW-130 photomultiplier coldbox was used every night except the

first, when a two-channel coldbox was used instead. Three filters were used to separate the first and second orders of the gratings, and an observation was made of each star in each filter. The effective wavelengths used for passbands per filter are: Filter 1 (3500Å, 3571Å, 3636Å, 4036Å, 4167Å, 4255Å), Filter 2 (4167Å, 4255Å, 4400Å, 4565Å, 4785Å, 5000Å, 5263Å), and Filter 3 (5263Å, 5840Å, 6300Å, 6710Å, 7100Å, 7780Å). Each passband within a filter set was measured twice, with the starting wavelength measured a total of 4 times. Note that three passbands (4167, 4255, and 5263Å) are observed in two separate filters. Multi-observations of a given filter are averaged together.

The passbands chosen are among the standard passbands of Oke (1964) and Hayes (1970) which give a fairly uniform distribution in  $1/\lambda$ . During 1973, all bandwidths for the observed passbands were 32Å. In 1974, the bandwidth for filters 1 and 2 (as defined above) were 48Å, while the bandwidth used for filter 3 was 64Å. Object observations were interweaved with sky observations for all stars. Hayes (1970) standard stars were also observed during most nights, sampling among all 12 Hayes standards with emphasis on observing  $\alpha$  Lyrae. At least 10,000 counts were accumulated at each passband for each star to obtain sufficient signal to noise.

## 2.2. Calibration

The first step in the data reduction (done in 1974) was the interpolation of the sky measurements to the time of observation of a given star, which was never significant at  $>1\%$  in the final magnitudes. Next, the observations for the Hayes standard stars and the cluster stars for each night were reduced using standard Mt. Hamilton extinction coefficients provided by E. J. Wampler.

One star from each cluster was measured several times during a given night (such stars are listed in Table 2 as the “secondary standard”) to internally standardize each cluster onto the same system. These stars were also used to determine any trend of atmospheric extinction different from the assumed coefficients during the night. Only during Night 3 was a deviation detected, affecting only the data for two stars (Per 285A, Per 383). In addition, we later discovered that two of the cluster secondary standard stars (Praesepe 300 and Coma 60) are Am stars, with one (Coma 60) suspected of being variable. Fortunately, we can explicitly test if use of these stars has affected the calibration of these two clusters (§ 3). To complete the standardization of the data, a smoothed energy distribution from the most-observed secondary standard star, Hya 56 (HD 27962), was used as the fundamental standard for all cluster stars. Lastly, each wavelength’s flux was normalized with respect to its flux value at 5556Å. We will therefore often refer to our fluxes as spectrophotometric

“colors.”

For the present paper these data are placed onto the spectrophotometry standard of the CSS. The data quoted in the CSS use a similar scanner-type system, and are standardized to the system of Hayes & Latham (1975). Of the eight stars in common, two are from Pleiades, four stars from the Hyades, and two Ap stars from Coma Berenices. As the data in the CSS for these stars only extends to 7100Å, we assume that our data for longer wavelengths will require the same zero point correction as for neighboring shorter wavelengths.

A systematic offset was indeed found between the 1974 reduction and the data of the CSS. This offset was easily quantified as being +0.005 mag for the 13 passbands  $> 4000\text{\AA}$ , and +0.037 mag for the three passbands at 3500–3636Å. The sense of both offsets is that our 1974 reduction produced fluxes too bright in the Hayes–Latham (1975) sense. Our zero point offsets are in the same sense as those known between the Hayes (1970) and Hayes–Latham (1975) systems. The correction for passbands  $> 4000\text{\AA}$  are consistent with that given by Hayes and Latham, while that for passbands in the UV are larger by about 0.02 mag. Such an offset likely arises from differences in the true atmospheric extinction from that assumed. Once corrected, the mutual scatter between our spectrophotometry and that of the CSS is  $\pm 0.016$  mag ( $1\sigma$  per color) averaged over all 15 colors, as seen in Figure 1a. We adopt these corrections, so that our data are formally on the spectrophotometric system defined by Hayes–Latham.

### 2.3. Comparison to Other Spectrophotometry

Our comparison with the two other spectrophotometric catalogs, SSA and BVJ, are done using our CSS-corrected data. We have three stars in common with the SSA: Pra 114, 154 and 276. As can be seen in Figure 1b, a color-by-color comparison yields relatively poor agreement,  $\pm 0.046$  per observation for all three stars. There are systematic offsets between our data sets that tend to divide into wavelength regimes above and below 5000Å.

A comparison with the spectrophotometry of BVJ is complicated by the fact that they calibrated their data to a different standard system than that of Hayes & Latham (cf. discussion in BVJ). As such, we have compared our data with those of BVJ as follows and summarized in Table 3: Column (1) gives the color bandpass for 15 colors (the 4400 color is not used). Column (2) is the difference in adopted zero point, BVJ - Hayes–Latham, calculated from the data given in Table 2 of BVJ. Column (3) is the mean raw difference, US – BVJ, with the error of the mean (i.e.,  $\sigma/\sqrt{N}$ ) for this raw difference given in Column

(4). Column (5) is the difference between column (3) and column (2), giving the observed minus the predicted zero point offsets (obs–pred) between our data and that of BVJ. For the three bandpasses below the Balmer jump, the offset in obs–pred is  $+0.0133 \pm 0.006$  mag (errors of the mean quoted); while above the Balmer jump it is  $-0.009 \pm 0.004$  mag. Overall the difference is only  $-0.005 \pm 0.004$  mag.

The difference, star-by-star, *after* the mean raw difference (US–BVJ) has been removed from the comparison, is shown in Figure 1c. Comparison with Figures 1a and 1b indicate that the scatter between our data that those of BVJ is larger than that with the CSS data, but smaller than that of Gunn & Stryker. A star-by-star comparison between BVJ and US indicates that most of the difference is systematic, cluster-by-cluster. For the three bandpasses below the Balmer jump, the mean difference, US–BVJ is  $-0.025$  mag for 5 Coma stars (with one star having a difference of  $-0.050$  mag),  $+0.024$  mag for 4 Praesepe stars (one star with  $+0.061$ , another  $+0.041$ ), but less than  $0.01$  mag for 5 stars in Hyades and 2 in Pleiades. Agreement is generally better for all clusters for the 12 bandpasses redward of the Balmer jump, with typical differences of  $0.01$ – $0.02$  mag, and no difference greater than  $-0.033$  mag.

Two stars have been observed by three data sets: Hya 95 by US, CSS and BVJ; and Pra 154 by US, SSA and BVJ. The three-way intercomparison is shown in Figure 1d. The agreement among US, CSS and BVJ for Hya 95 is reassuring, showing scatter per observation of less than  $0.01$  mag. However, it is clear from comparing US vs. BVJ and BVJ vs. SSA for Pra 154 that none of the observations are in good agreement with the other, although BVJ seem to agree a little better with SSA than US with BVJ.

Why we agree better with CSS than BVJ or SSA is not obvious. Of the 8 stars in common with CSS, all are in the same clusters as used in comparing to BVJ (Coma, Hyades, Pleiades). BVJ observed some of their stars in common with us on more than one night, others just on one night (as in the present survey). The “usual” suspects — errors in nightly extinction or nightly zero points, variable stars, just bad luck with random statistics — are likely, but not proven. Fortunately, we have other means of assessing the accuracy of our data (§ 3, § 4, § 5) that include most of the stars in our sample. As a result, we defer a final discussion of the errors of our spectrophotometry until all comparisons are made.

## 2.4. The Calibrated Data

The final calibrated spectral energy distributions (SEDs; relative to  $5556\text{\AA}$ ) for all 237 stars are given in Table 4 according to the cluster identification number and the night(s) of

the observation. The source of cluster identification number is given in the Table notes. A colon is placed after values with *a priori* known estimated errors of  $\sim 0.03$ – $0.06$  mag; an asterisk indicates errors  $> 0.06$  mag (which were usually interpolated from adjacent wavelengths). This table will also be made electronically available as described at the end of this paper.

## 2.5. Cluster Color–Magnitude Diagrams

The SIMBAD database was searched to obtain  $V$  magnitudes, UBVRI colors, *wby* colors and spectral types for the stars. From these data we construct up-to-date color–magnitude (C–M) diagrams for the stars in these clusters that are in our survey (Figures 2a–g). Also plotted in the cluster C–M diagrams is the fiducial zero age main sequence (ZAMS) from Mihalas & Binney (1981), adjusted to match the least-evolved main sequence stars as well as possible. Based on this adjustment, some of the distances given for the clusters in Table 1 have been modified, as noted in that table. The ZAMS is useful for identifying likely main sequence stars for the comparison with Kurucz models (§ 4), and for detecting spectral type misclassifications (Appendix A). The stars specifically identified in Figure 2 will be discussed in Appendix A and elsewhere in the paper; stars used as secondary flux standards are noted with bold numbering.

We initially assume that luminosities and spectral classes of stars are as given by the MK types from SIMBAD. However, as can be seen in Figure 2, not all stars have MK classifications that correspond well to their position in the C–M diagram. We therefore modify our assumptions such that any star which could be sensibly defined as a main sequence star based on its position in the cluster C–M diagram was treated as such. Separately, most of the clusters appear to have a binary star population as evidenced by the stars lying parallel to, but offset from the ZAMS line.

## 3. Comparison of Spectrophotometry to Filter Color Systems

The spectrophotometry colors can be used to synthesize the filter colors of the Strömrgren *wby* and Johnson BV systems (cf. Breger 1976; Adelman 1981). For Strömrgren colors, two adjacent bandpasses are averaged to achieve a closer approximation to the filter effective wavelength. In the case of the Johnson BV filters, a convolution was made between these data and the B and V sensitivity functions ( $S(\lambda)$ ) defined by Matthews & Sandage (1963) such that:

$$(B - V)_1 = 2.5 \times \log \frac{\int_0^\infty S_V(\lambda)_1 F(\lambda) d\lambda}{\int_0^\infty S_B(\lambda)_1 F(\lambda) d\lambda}. \quad (1)$$

$F(\lambda)$  represents the flux taken from the present data and the subscript of 1 indicates that the sensitivity functions with an airmass of 1 were used to determine the B-V color. Table 6 list the observed B-V and *uvby* data as obtained from SIMBAD, together with the differences (observed minus predicted) between the colors we predict from our spectrophotometry and the observed colors. We will find these color “residuals” quite valuable in assessing the accuracy of our data (below and § 5).

The transformations between our spectrophotometry and the filter colors are given in Table 5, together with the results from a simple linear fit between predicted colors and observed colors. As all of our colors imply a magnitude difference of the given passband with the flux at 5556Å, the synthesized indices can be simply defined. Seventeen stars do not have *uvby* data. Seven stars were found to have significant residuals ( $> 3\sigma$ ) with respect to the *uvby* color fits: Com 65 (v-y; u-b); Com 162 (b-y); Com 183 (v-y; b-y); IC4 83 (b-y); IC4 89 (u-b; b-y); Per 285A (b-y) and Ple 2181 (a known variable star; v-y; u-b). The color residuals for these stars are foot-noted in Table 6, and these colors are not used to defined the transformation between the spectrophotometry and the filter colors.

The residuals, in the sense (observed-predicted) are given in Figures 3a,b,c,d, with stars from the different clusters denoted by different symbols. All the comparisons have a slope near unity, with deviations of  $\pm \sim 0.05$  mag from linearity in the color range -0.35 to -0.50 with B-V and in the range of -0.25 to -0.50 with *v-y*. Such deviations are not surprising, given the avoidance of strong absorption features by the spectrophotometry bandpasses, and the known sensitivity of the filter indices in the wavelength region 4000–4900Å to changes in helium and hydrogen absorption in this temperature range. The fact that we see little deviation in linearity in the *u-b* comparison is a testament to the strong line blocking below the Balmer jump which makes any filter in this wavelength range sensitive to absorption features.

Regarding the two clusters whose secondary stars are suspected variables, Praesepe and Coma Berenices, we find that their stars follow the average filter-SED *b-y* correlation to 0.001 mag and -0.001 mag, respectively, with scatter of 0.015 and 0.017 mag ( $1 - \sigma$ ). This is quite comparable to the zero points and scatter found for the other 5 clusters (a range in zero point from -0.0004 to +0.0027 and scatter from 0.010 to 0.018 mag). Similarly, we find Praesepe and Coma Berenices stars to follow the filter-SED *u-b* zero point to 0.004 to 0.01 mag, with scatter of 0.026 and 0.021 mag, respectively. Again, this is comparable to what we find for the stars in the other 5 clusters (zero points from 0.001 to -0.010 mag; scatter



from 0.017 to 0.031 mag). Thus, we can find little evidence that the secondary standard stars varied sufficiently during the period of observation to differentially affect the SEDs of the stars in these clusters at a level we can detect.

Given the obvious non-linearity in the relation with  $v-y$  and B–V, our preliminary estimate of the accuracy of our photometry from the filter comparison comes from the fits to  $u-b$  and  $b-y$ , which sample a comparable range in wavelength as the other two colors. As shown in Table 5, we get a  $(1 - \sigma)$  scatter of 0.023 mag for  $u-b$  and 0.013 mag for  $b-y$ . The implied scatter for our data (0.01–0.02) mag compares favorably with the estimate we get from comparing to the CSS, but is clearly smaller than our comparisons to BVJ and the SSA. Lines of  $\pm 0.015$  mag are drawn in Figure 3 to guide the eye relative to the scatter seen.

## 4. Comparison to Kurucz Models

### 4.1. The Kurucz Models

The stellar synthesis models of Kurucz (e.g., 1979, 1992, 1993) have been widely used over the years, especially as Kurucz has strived to improve their relationship to real stellar spectra. For example, Adelman (1981) used Kurucz (1979) models to estimate temperatures and gravities for certain stars in the CSS. We believe that by comparing the models of Kurucz (1993) to our data, we are making one of the more comprehensive comparisons of spectrophotometry between models and stars with a large range in temperature. As will be seen, we also benefit from this comparison, as the models give us an estimate of the accuracy of our spectrophotometry that is both more extensive and independent of the filter colors, and more comprehensive than intercomparisons with other observers (§ 2, § 3).

We opt to explore only the variation of temperature with respect to the Kurucz models for the stars in our sample for two reasons. First, the differences in  $[\text{Fe}/\text{H}]$  from solar are at the 0.1 dex level for these clusters. Second, likely gravity differences among upper main sequence stars of ages 30–1000 Myr are generally less than 0.5 dex, at the resolution of the grid of models provided by Kurucz. Rather than interpolate among the Kurucz models for relatively small gravity and metallicity differences, we choose instead to explicitly test for evidence of such differences. We compare our data to Kurucz models with  $[\text{Fe}/\text{H}] = 0.00$ ,  $\log g = 4.0$  and a microturbulent velocity of  $2 \text{ km sec}^{-1}$ . A spectral resolution of  $32\text{\AA}$  resolution was assumed for this comparison, as most of the data were taken with this resolution. We take into account the reddening of each cluster by appropriately reddening the Kurucz models for the stars in each cluster, using the  $E(\text{B}-\text{V})$  values given in Table 1

and a standard Seaton (1979) reddening curve.

## 4.2. Ordering of Stellar SEDs by Cluster and Temperature

We compare the Kurucz models to all stars in our data which we classify as main sequence stars either based on their spectral classification or by their placement in the cluster C–M diagrams (§ 2.5). The best-fit Kurucz model to the data is chosen by comparing the full range of Kurucz models with  $[\text{Fe}/\text{H}] = 0.0$ ,  $\log g = 4.0$  and varying temperature. For each model comparison we calculate a least squares fit parameter  $s$ , defined as  $s = \frac{\sqrt{\sum_{13} res^2}}{13}$ , where  $res$  is the difference between our flux and that of Kurucz only for the 13 passbands with  $\lambda > 4000\text{\AA}$ ; i.e., above the Balmer jump. The minimum of this distribution for the residual sum is taken to be the appropriate temperature model. For this comparison we specifically exclude the 3 bluest spectrophotometric colors for the well-known reason that gravity and metallicity effects are far larger for colors defined by combining passbands above and below the Balmer jump, relative to colors defined where both passbands are above the Balmer jump. Rather, based on the best fit to the model for the wavelengths above the Balmer jump, two separate average residuals (obs–model) are calculated for each star; one for the 13 “red” colors and one for the 3 “blue” colors.

In this process we do not *a priori* require that the mean (obs–model) residual for each cluster be exactly zero. Rather, by letting this value float freely, we provide an extra check on the accuracy of our comparison. As expected, the average difference per cluster, (obs–model) for the 3 “blue” colors shows significant scatter (see also below). Despite that scatter, significant zero point offsets (at  $> 5\sigma$  significance) of  $-0.013$  and  $-0.017$  mag are found only for the Hyades and Praesepe clusters. Since these clusters are the oldest in our sample, somewhat metal-enhanced (Table 1), and with cooler stars whose SEDs are more affected by metallicity, such a small difference is not surprising given our use of solar metallicity models. Interestingly, zero point differences at  $\leq 0.01$  mag level are also seen for the average of 13 “red” colors for Hyades, Pleiades, Coma Berenices and IC 4665 stars.

Figures 4a–g show the SEDs for the main sequence stars in each cluster, grouped according to their best-fit Kurucz temperature. For the most part, the stars of similar temperature have SEDs that match well (indicating that the comparison worked), with the largest differences in the  $3500\text{--}3636\text{\AA}$  range, as expected. Figure 5 shows the SEDs of the non-main sequence stars (luminosity classes I, III, and IV) which were not explicitly compared to Kurucz models, grouped according to SED.

### 4.3. Gravity and Other Effects in the Kurucz Comparison

Figures 6a,b graph the absolute V magnitudes of the stars in our sample (using our predicted distances and reddenings) versus the residuals (observed–predicted) for the fit of Kurucz models to our data, with the known (small) zero point differences removed. Figure 6a plots  $M_V$  versus the blue color residuals; Figure 6b plots  $M_V$  versus the red color residuals. Note the difference in plotting scale used for the residuals in Figure 6a versus that used in Figure 6b.

As would be expected, the scatter of the Kurucz models versus the 13 red colors of our spectrophotometry show no residual dependence on absolute magnitudes, with an average scatter ( $1 - \sigma$ ) of 0.01 mag per star (Figure 6b). As equally expected, the scatter of the Kurucz models versus the 3 UV colors shows highly systematic differences as a function of stellar absolute magnitudes. The most obvious effect is that gravity differences among the upper main sequence and subgiant stars strongly affect the UV residuals. This is to be expected.

More interesting, perhaps, are the more subtle differences among the red color residuals for the lower main sequence stars. In the range  $3.0 < M_V < 2.5$  are seven Hyades stars that progressively deviate from the Kurucz models with brighter magnitudes (#’s 38,45,53,68,80,94,103). Of these stars, two are known Am stars, one is classified as a subgiant (!), and the others are either F0V or F4V. It is possible that these small, but systematic differences are caused by increased line absorption symptomatic of the Am phenomenon (might this also be the source of the apparently mis-applied subgiant classification?), rather than variability, as no similar variation is seen for the red colors of these stars. Separately, stars fainter than  $M_V = 4.5$  in both Hyades and Coma show a somewhat wider spread in red residuals than do brighter main sequence stars in these two clusters. Why this latter effect is so is not clear, as a gravity effect alone should produce a net shift in the residuals, rather than a wider range. Perhaps some of the stars are low mass-ratio binaries, which could effect the model comparison only in the reddest colors?

## 5. A Quantitative Assessment of Spectrophotometry Errors for Individual Stars

The quantitative comparisons among our spectrophotometry, the CSS spectrophotometry, the *wby* and B–V colors, and the Kurucz models all indicate an accuracy for our spectrophotometric colors of 0.01 - 0.02 mag,  $1 - \sigma$ . Yet, in quoting  $1 - \sigma$  errors, we realize that in a data set as large as ours,  $2 - \sigma$ ,  $3 - \sigma$  and even greater errors must exist

if the distribution of errors is Gaussian. As these data can be useful in accurately defining spectral energy distributions of bright stars for use in stellar population models and for calibrating CCD images, it is highly desirable that the photometric accuracy for the SED of each star be known.

Fortunately, most of the stars in our sample have both *ubvy* colors and residuals from the Kurucz models. Suppose that the Kurucz models define accurate spectral energy distributions for stars in the wavelength region we have sampled *and* the errors in the *ubvy* filter colors are small and uncorrelated with our spectrophotometric errors. If both statements are true, if we plot the (observed-filter) residuals to the *ubvy* colors ( $\delta(\text{color})$ ) versus the (observed-model) residuals to the Kurucz models ( $\delta(\text{Model})$ ), these residuals should be strongly correlated.

Figure 7a shows the correlation of  $\delta(u - b)$  with  $\delta(\text{Blue Model})$ ; Figure 7b the correlation of  $\delta(b - y)$  with  $\delta(\text{Red Model})$ . The term Red Model applies to the mean residuals for the 13 red colors; similarly, the term Blue Model applies to the mean residuals for the 3 UV colors. In the case of the  $\delta(b - y)$  vs.  $\delta(\text{Red Model})$  a clear correlation exists. For 198 stars with (b–y) colors, Kurucz model fits and not otherwise large color residuals, the correlation coefficient between  $\delta(b - y)$  and  $\delta(\text{Red Model})$  is 0.55 with a  $1 - \sigma$  scatter of 0.011 mag. For the 132 stars with  $M_V \geq 1.00$  and with good predicted (*u–b*) colors, the correlation coefficient between  $\delta(u - b)$  and  $\delta(\text{Blue Model})$  is 0.298 with a  $1 - \sigma$  scatter of 0.023 mag.

The fact that we see significant correlations between the color residuals and the model residuals means that the above hypothesis is reasonably correct: In comparing to the filter colors and the Kurucz models, we see mainly the errors in the spectrophotometric colors, while the errors in the filter colors and the models are much smaller than these. As a result, we have chosen to tabulate the values of  $\delta(u - b)$ ,  $\delta(v - y)$ ,  $\delta(b - y)$ , and  $\delta(B - V)$ ,  $\delta(\text{Blue Model})$  and  $\delta(\text{Red Model})$  for those stars with requisite data in Table 6, rather than the predicted filter colors. Inspection of the values of  $\delta(b - y)$  and  $\delta(\text{Red Model})$  in particular are useful in choosing stars from our sample with the most accurate spectrophotometry. The other color residuals and  $\delta(\text{Blue Model})$  are also somewhat useful in this regard as a cross-check.

Given this conclusion, it is reasonable to interpret the scatter in the correlation of the residuals in Figure 7 as due primarily to the errors in the spectrophotometric colors. This means that one can use the size of the color and Kurucz residuals to reliably estimate the accuracy of the SED of each star, taking  $1 - \sigma$  errors of 0.01 mag for the red colors, and 0.023 mag for the blue colors as the starting point. Separately, we find these error estimates consistent with our estimated errors from our spectrophotometric comparison with CSS,

but significantly smaller than our comparisons to SSA (0.046 mag) and BVJ (up to 0.03 mag) (§ 2.3).

## 6. Summary

We present spectrophotometric data in 16 bandpasses from 3500 – 7800Å for 237 stars in seven nearby open clusters which range in age from 30 to 900 Myr: Hyades, Pleiades, Coma Berenices,  $\alpha$  Persei, Praesepe, IC 4665 and M39. These data are presented in the form of spectrophotometric colors (color  $\lambda = \lambda_{5556} - \lambda$ ). Absolute calibration of the colors is done by comparing our data with those of Adelman et al. (1989) for eight stars in common. External comparisons are then done with respect to other published spectrophotometry, *uvby* colors, B–V colors and the predicted spectral energy distributions of Kurucz (1993) models.

Both the filter color comparison and the comparison to Kurucz models yield accuracy estimates for our spectrophotometry consistent with what we find in our comparison with Adelman et al.: a  $1 - \sigma$  accuracy of 0.01 mag for the 13 colors formed with passbands redward of the Balmer jump, and 0.023 mag for the 3 UV colors. In contrast, comparison to the published spectrophotometry of Gunn & Stryker (1983) and Bohm-Vitense & Johnson (1977) indicates larger errors (0.03 - 0.045 mag).

The comparison to Kurucz models was made for main sequence stars with values of log gravity and [Fe/H] fixed at 4.0 and solar, respectively. Gravity differences and absorption line differences among the stars, more finely than can be measured with the standard Kurucz grid, are seen when residuals (obs minus model) are separately tabulated for the 3 UV colors and the 13 red colors. While the residuals for the red colors show no net gravity effect, the UV colors show a strong gravity effect, as would be anticipated from colors that measure the strength of the Balmer jump in B-F stars.

We show that it is reasonable to assume that, compared to the spectrophotometric errors, the errors in  $(u-b)$ ,  $(b-y)$  and the Kurucz models are small, so that the residuals  $\delta(u - b)$  are correlated with the Kurucz UV residuals ( $\delta(\text{Blue Model})$ ), and the residuals  $\delta(b - y)$  are correlated with  $\delta(\text{Blue Model})$ . These residuals can be used to identify those stars for which the spectrophotometric colors are the most reliable, and those which are less reliable. Thus, while we quote  $1 - \sigma$  accuracies for our data, we can also determine which stars have spectrophotometry within  $1 - \sigma$  accuracy,  $2 - \sigma$ , etc. This list should therefore be valuable to those who would like to have accurate spectrophotometric color standards for calibration of imaging and spectroscopic data.

Table 4 and Table 6 will be made electronically accessible via both anonymous ftp (samuri.la.asu.edu = IP #129.219.144.156) and through the Astronomical Data Center.

These data would not exist without the hard work and perserverence of Lee McDonald, for which we sincerely thank him. LC was supported in part by a NASA Space Grant assistantship; DB was supported in part by NASA Grant GR 6309.194A. We thank Linda Stryker and Per Aannestad for helpful suggestions. We also thank the anonymous referee for perceptive comments on the first version of this paper that were particularly helpful. The SIMBAD database was used to obtain much useful data for these stars.

### A. Discussion of the Peculiarities Individual Stars

A number of stars are noteworthy in terms of how their MK classifications and SEDs correspond to their positions in the C–M diagrams (Figure 2). We discuss these stars on a cluster-by-cluster basis.

**Hyades:** Hya 126 (= HD 31236) falls below the main sequence despite being classified F3 IV. While its predicted temperature,  $\sim 7500$  K, is consistent with an F classification, its SED gives one of the worst comparisons to the Kurucz models. Hya 112 (= HD 30210) has one of the best comparisons to Kurucz models, but also appears a bit underluminous for its color. As this star is classified Am, possible variation in color and magnitude could produce such an effect. Hya 72 (= HD 28319) lies well above the main sequence and is classified as A7III. Yet, its SED is similar to those of main sequence stars of similar temperature, such that this star was included in the Kurucz comparisons. Hya 72 could be a blue straggler, given its position relative to the main sequence turn-off.

**Pleiades:** Ple 563 (= HD 23338), classified B6IV, has an SED that is in very good agreement with the other subgiants in this cluster at wavelengths above  $4000\text{\AA}$ , but is significantly more luminous below the Balmer jump. Ple 2181 (= HD 23862) is a known variable which affects its filter color comparisons. Ple 1375 (= HD 23629, A0V) has a similar estimated temperature as Ple 817 (= HD 23432, B8V), despite being both redder and less luminous in the C–M diagram (cf. Figure 2b). These two stars also differ significantly in their fluxes below the Balmer jump, with Ple 1375 being 0.3 mag redder than Ple 817. As the SED of Ple 817 is more in accord with Kurucz models, this would indicate Ple 1375 is a likely binary, consistent with its offset position from the main sequence.

**Praesepe:** Pra 265 (= HD 73666) is significantly bluer than, and offset from, the well-defined main sequence of this nearly 1 Gyr old cluster. With an F6V classification

it could either be an interloper in the cluster, or a blue straggler. Separately, five of the stars in our sample are nominally classified as giant stars, but clearly lie within the evolved main sequence of this cluster (224 = HD 73618; 276 = HD 73711; 279 = HD 73709; 292 = HD 73729; and 328 = HD 73785). These must either be misclassifications or non-member interlopers. Pra 142 (no HD number) and Pra 275 (no HD number) are among the faintest and coolest main sequence stars in our sample. They are also likely binary stars, as they lie well above the fiducial single star main sequence of this cluster. This is consistent with the SED comparison to Kurucz models, which implies the SEDs of these two stars are different from those of a single star.

**$\alpha$  Persei:** Most of stars in this cluster are classified as Ap. Per 868 (= HD 21479) is classified as A1IV yet it lies near the main sequence (Figure 2d). Of the five most luminous stars extending above the main sequence (not counting Per 605, a supergiant), only one is formally classified as a peculiar giant (Per 985 = HD 21699, B8IIImp). All of the other stars at the tip of the evolved main sequence are classified as main sequence, B3–B6, with one being B6Vn.

**Coma Berenices:** One third of the stars in this cluster are classified as A-peculiar (p, n or m), the largest fraction of any of the seven clusters. Two of the stars in common with CSS (Com 146 = HD 108662 and Com 160 = HD 108945) are noted by Adelman (1981) as being variable. Others are noted as variable in the SIMBAD data base. The two obvious evolved stars in this cluster (Com 125 = HD 108283 and Com 91 = HD 107700) do not have luminosity classifications. Interestingly, the SED of Com 91 (F2) matches well with the SED of the supergiant star Per 605 (F5Iab), despite being in very different positions relative to the main sequences in their respective clusters.

**IC 4665:** This cluster has the most poorly-defined main sequence of any of these seven clusters. It is not *a priori* clear whether the scatter along the main sequence is due to a strong binary star population, poor data or field star contamination. One star, IC4 83 (no HD number) is defined as a double system by SIMBAD, but is not otherwise much offset in the C-M diagram from the nominal single star main sequence.

**M39:** Only nine stars are observed in M39, the fewest of any cluster in our sample. Three of the 6 main sequence stars are classified Ap.

## REFERENCES

- Adelman, S. J., et al. 1989, A&AS 81, 221 (CSS)
- Adelman, S. J. 1981, A&AS 43, 25
- Adelman, S. J. 1979, AJ 84, 857
- Alter, G., Ruprecht, J. & Vanysek, V. 1958, Catalogue of Star Clusters and Associations, (Czechoslovak Academy of Science: Prague)
- Ardeberg, A. & Virefors, B. 1980, A&AS 40, 307
- Breger, M. 1976, ApJS 32, 7
- Bohm-Vitense, E. & Johnson, P. 1977, ApJS 35, 461 (BVJ)
- Crawford, D. L. & Barnes, J. V. 1972, AJ 77, 862
- Ebbinghausen, E. G., 1940, ApJ 92, 434
- Gunn, J. & Stryker, L.L. 1983, ApJS 52, 122 (SSA)
- Hayes, D. S. 1970, ApJ 159, 165
- Hayes, D. S. & Latham, D. W. 1975, ApJ 197, 593
- Heckmann, O., Dieckvoss, W., & Kox, H., 1956, A. N. 283, 109
- Hertzsprung, E., 1947, Ann. Leiden Obs. 19, No. 1A
- Klein-Wassink, W. J., 1927, Groningen Publ. No. 41
- Kopff, 1943, Mitt. Hamburg Stw. 8, 52
- Kurucz, R.L. 1979, ApJS 40, 1
- Kurucz, R. L. 1992, in Stellar Populations of Galaxies, IAU Symp 149, eds. B. Barbuy & A. Renzini, (Kluwer: Dordrecht), p. 227
- Kurucz, R. L. 1993, CD-ROM 13 release
- Lynga, G. 1987, Lund-Strasbourg Catalogue, 5th Edition (Uppsala Obs: Uppsala)
- Matthews, T.A. & Sandage 1963, ApJ 138, 30
- Mendoza, E. E. 1967, Bol Ton y Tac 4, 149
- Mihalas D. & Binney J. 1981, Galactic Astronomy, (Freeman & Co.: New York), p. 106
- Oke, J. B. 1964, ApJ 140, 689
- Oke, J. B. & Schild, R. E. 1970, ApJ 161, 1015
- Seaton, M. 1979, MNRAS 187, 73



Trumpler, F. J., 1938, Lick Obs. Bull. 18, 167

Van Bueren, 1952, B. A. N. 11, No. 432

Wampler, E. J. 1966, ApJ 144, 921

## Figure Captions

**Figure 1.** (a) A comparison of the SEDs of eight stars to the data in the Catalogue of Stellar Spectrophotometry (Adelman et al.). The stars used are identified in the legend, and the residuals are in magnitudes. Dotted lines are drawn at  $\pm 0.015$  residuals for guidance. (b) A comparison of the SEDs of three stars to the data of the Stellar Spectrophotometry Atlas (Gunn & Stryker). Note the much larger scatter, both random and systematic, in (b) than in (a). (c) A comparison of the SEDs of 16 stars in common with the data of Bohm-Vitense & Johnson. Here the scatter is intermediate between (a) and (b). (d) A three-sided comparison of spectrophotometry for two stars observed by three separate observers. Stars and observers noted in the figure.

**Figure 2.** V vs. (B–V) color-magnitude diagrams for the stars observed in each cluster. Stars are distinguished by MK spectral type (see figure legend) where available or by estimated luminosity classes based on their positions in these diagrams. Specific stars of interest that are discussed in the text are indicated using the cluster numbers given in Table 5. The Zero-Age-Main-Sequence from Mihalas & Binney (1981) is also given in each C-M diagram for guidance. (a) Hyades; (b) Pleiades; (c) Coma Berenices; (d)  $\alpha$  Persei; (e) Praesepe; (f) IC 4665 and (g) M39.

**Figure 3.** The residuals of linear fits of ( $u-b$ ) (a), ( $b-y$ ) (b), ( $v-y$ ) (c) and (B–V) (d) colors with equivalent estimates from the SED data. The fits used are given in Table 4. Data for stars from different clusters are plotted with different symbols, as given in the legend. Residuals are plotted in the sense of (observed minus SED).

**Figure 4.** The SEDs of the main sequence open cluster stars, arranged by cluster and within clusters, matched by similar temperatures as indicated by the comparison with Kurucz models. In contrast to the other figures, the SEDs are plotted here as flux ratios, rather than as magnitudes. Stars in each group are identified, as well as estimated temperature range of the stellar grouping.

(a) Hyades: 8750K (56), 8000K–8250K (47,72,82,95,112,54,104,108),  
 7500K–7750K (24,30,55,60,67,83,84,111,126,141,74,123),  
 7000K–7250K (11,20,32,53,100,38,45,68,80,89,103), 6750K (34,35,36,44,51,78,85,94,101,128),  
 6500K (57,77,81,86,121,124), 6250K (29,31,40,48,52,59,62,65,66,75,88,105,118,119,146),  
 5750K–6000K (23,39,50,73,97,102,106,58).

(b) Pleiades: 14000K–15000K (1823,541), 12000K–13000K (859,2263,2425),  
 11000K–11500K (1375,817), 9750K–10500K (801,1234,1380),  
 9000K–9250K (1028,2220,2866,1397,1431), 8500K–8750K (717,1425,2289,153,1876),

8250K (232,804,1384,2415), 7250K–8000K (157,1084,344,1407,2195).

(c) Praesepe: 9750K (265), 8000K–8250K (50,114,207,224,279,328,284,300,348,375,445,276), 7750K (45,143,203,229,204), 7500K (150,154,284,292,340), 6750K–7000K (227,239,146), 6250K–6500K (142,275,268).

(d)  $\alpha$  Persei: 16000K–20000K (557,675,774,835), 14000K–15000K (383,810,955,904), 12000K–12500K (831,735), 11000K–11500K (581,1082,692), 9500K–10000K (423,868,612,775), 9250K (167,575,639,756,817,875), 8500K–9000K (651,780,386,625), 8000K (285A).

(e) Coma Berenices: 10000K (146), 8500K–9000K (10,130,107,160), 8000K (60,62,68,139,144), 7500K–7750K (82,109,104,145), 7000K(19,36,49), 6750K (86,90,101,118,183), 6500K (53,58,65,114,162), 6250K (76,85,97,111).

(f) IC 4665: 19000K (58), 16000K–17000K (49,73,62,105), 13000K–15000K (82,23,32), 10000K–11500K (81,102,22), 9500K–9750K (43,76), 8500K–8750K (27,50,83,67,89), 8000K–8250K (63,118,39,66), 7500K–7750K (65,51).

(g) M39: 11000K (26), 10500K (1,23), 10000K (33,40A), 9750K (24,38), 9500K (5,17).

**Figure 5.** The SEDs of the non-main-sequence stars in our data set, plotted as a function of approximate ascending temperature. Note the similarity of the SEDs of Com 91 and Per 605, despite their difference in MK classification (Appendix A).

**Figure 6.** The relation of absolute V magnitude with the residuals from the fit of Kurucz  $\log = 4$ ,  $[\text{Fe}/\text{H}] = 0.00$  model to the SEDs in which only temperature is varied. (a) The average of the 3 UV colors, termed “blue model residuals;” (b) The average of the 13 red colors, termed “red model residuals.” Note that the y-axis scale is 6.5 smaller for (b) than for (a). Symbols for different cluster stars as in Figure 3.

**Figure 7.** The residuals of predicted *uvby* colors plotted versus the model residuals from the Kurucz model fits. (a)  $\delta(u - b)$  versus the “blue model residuals.” (b)  $\delta(b - y)$  versus the “red model residuals.” Lines drawn are the average fit obtained by interchanging X and Y parameters and taking the average of the fits. Symbols for different cluster stars as in Figure 3.

Table 1: Table of Selected Clusters

Cluster Name	Other Name	l <sup>a</sup> (deg)	b <sup>a</sup> (deg)	d <sup>b</sup> (pc)	log age <sup>b</sup> (yr)	E(B-V) <sup>b</sup>	[Fe/H] <sup>b</sup>
Praesepe	M44	205.5	+32.5	160/180 <sup>c</sup>	8.92	0.03	+0.07
Hyades	...	180.1	-22.4	43	8.85	0.00	+0.12
Coma Berenices	Mel 111	221.1	+84.1	80/90 <sup>c</sup>	8.66	0.00	-0.03
M39	NGC 7092	92.5	-2.3	290	8.30	0.06	...
Pleiades	M45	166.6	-23.5	130/180 <sup>c</sup>	8.11	0.06	+0.12
IC 4665	...	30.6	+17.1	340/470 <sup>c</sup>	7.89	0.17	...
$\alpha$ Persei	Mel 20	147.0	-7.1	160/230 <sup>c</sup>	7.61	0.10	+0.10

---

<sup>a</sup>Data taken from Alter, et al (1958)

<sup>b</sup>Data taken from 5th Ed. of Lund-Strasbourg Catalogue (1987)

<sup>c</sup>These distances are adjusted from the placement of the ZAMS line (§2)

Table 2: Table of Observations

No.	Date	Clusters observed	Standard Star(s)
1	July 17/18, 1973	M39	M39 33
2	Aug. 14/15	Pleiades	Ple 785
3	Aug. 15/16	M39, $\alpha$ Persei	Per 605
4	Sept. 15/16	Pleiades	Ple 785
5	Sept. 16/17	Hyades	Hya 56
6	Sept. 17/18	$\alpha$ Persei,Pleiades	Ple 785
7	Sept. 18/19	Pleiades	Ple 785
8	Sept. 20/21	Hyades	Hya 56
9	Oct. 12/13	Hyades	Hya 56
10	Oct. 13/14	Hyades	Hya 56
11	Mar. 8/9, 1974	Hyades,Praesepe,Coma B.	Hya 56
12	Mar. 9/10	Coma B.	Com 60
13	Apr. 10/11	Praesepe	Pra 300
14	May 6/7	Coma B.	Com 60
15	May 7/8	Praesepe,Coma B.,IC 4665	Pra 300,Com 60
16	Aug. 9/10	IC 4665	IC4 62
17	Dec. 29/30	Hyades,Pleiades, $\alpha$ Persei	Hya 56

Table 3: Comparison to Bohm-Vitense–Johnson Calibration

Passband	BVJ Calib	Mean(US–BVJ) (obs)	Mean Error	Obs–Pred
3509	0.047	0.071	0.0100	0.024
3571	0.040	0.053	0.0086	0.013
3636	0.025	0.028	0.0075	0.003
4032	0.016	-0.005	0.0067	-0.021
4167	0.017	-0.013	0.0055	-0.030
4255	0.012	-0.006	0.0006	-0.018
4566	0.002	0.011	0.0067	0.009
4785	0.013	0.023	0.0056	0.010
5000	0.012	-0.014	0.0072	-0.026
5263	0.012	-0.006	0.0035	-0.018
5882	0.000	0.001	0.0034	-0.001
6370	-0.003	-0.004	0.0054	-0.001
6800	-0.006	-0.001	0.0054	0.005
7100	0.002	0.005	0.0033	-0.003
7850	0.003	-0.014	0.0074	-0.017

Table 5: Synthetic Passbands Used to Match Filter Color Systems

System	Color	Synthetic Indices	m	b	$\sigma$
Johnson	B-V	Matthews & Sandage (1963)	1.072	0.433	0.021
Strömgren	<i>u-b</i>	$3500 - (4565+4785)/2$	1.005	0.125	0.024
Strömgren	<i>b-y</i>	$(4565+4785)/2$	0.934	0.153	0.013
Strömgren	<i>v-y</i>	$(4036+4167)/2$	0.891	0.415	0.032

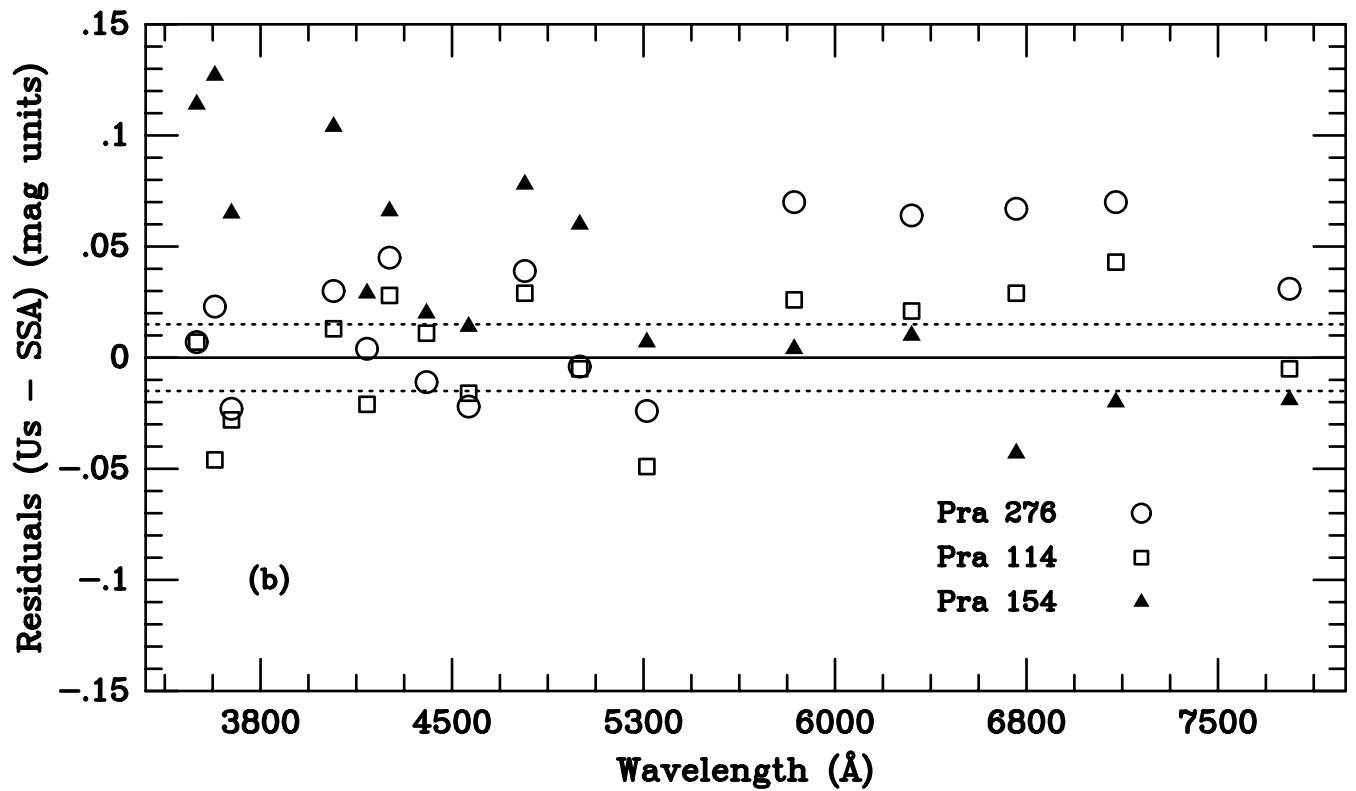
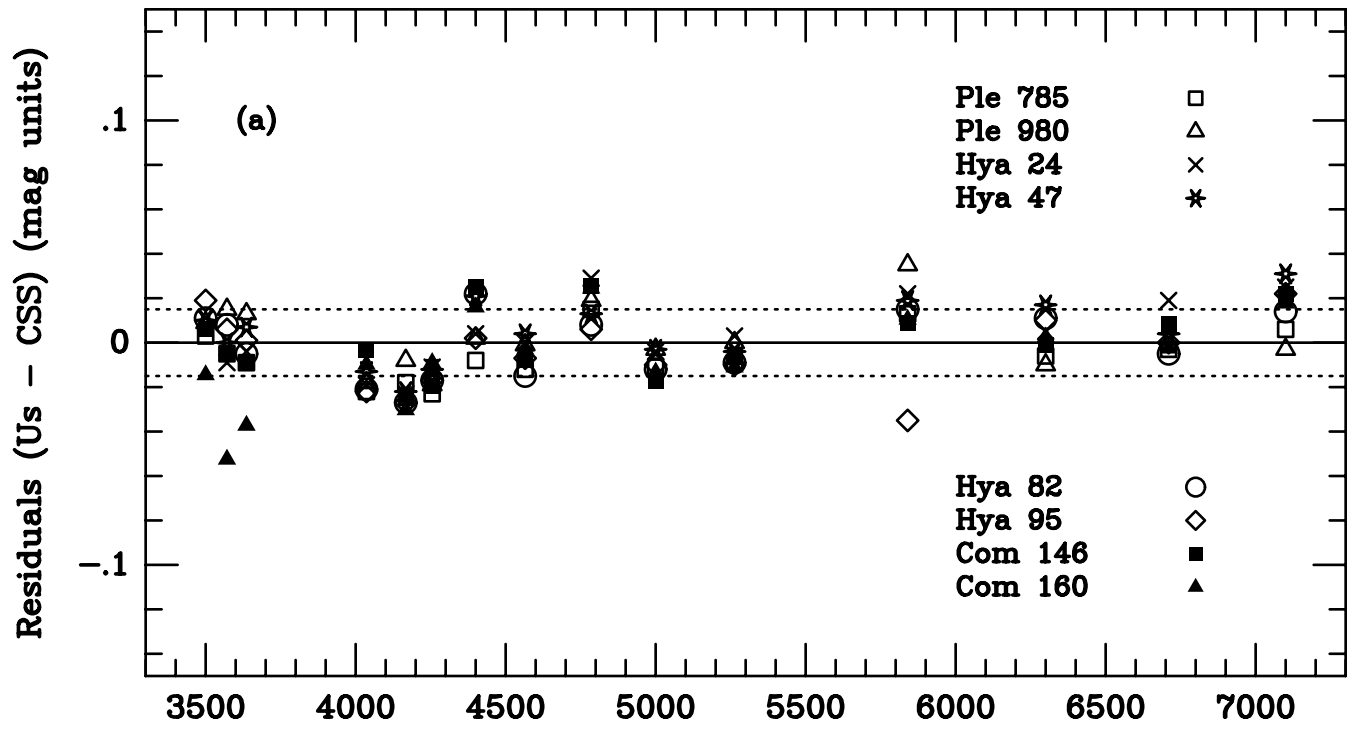


Figure 1a,b  
 Clampitt &  
 Burstein  
 AJ 1997



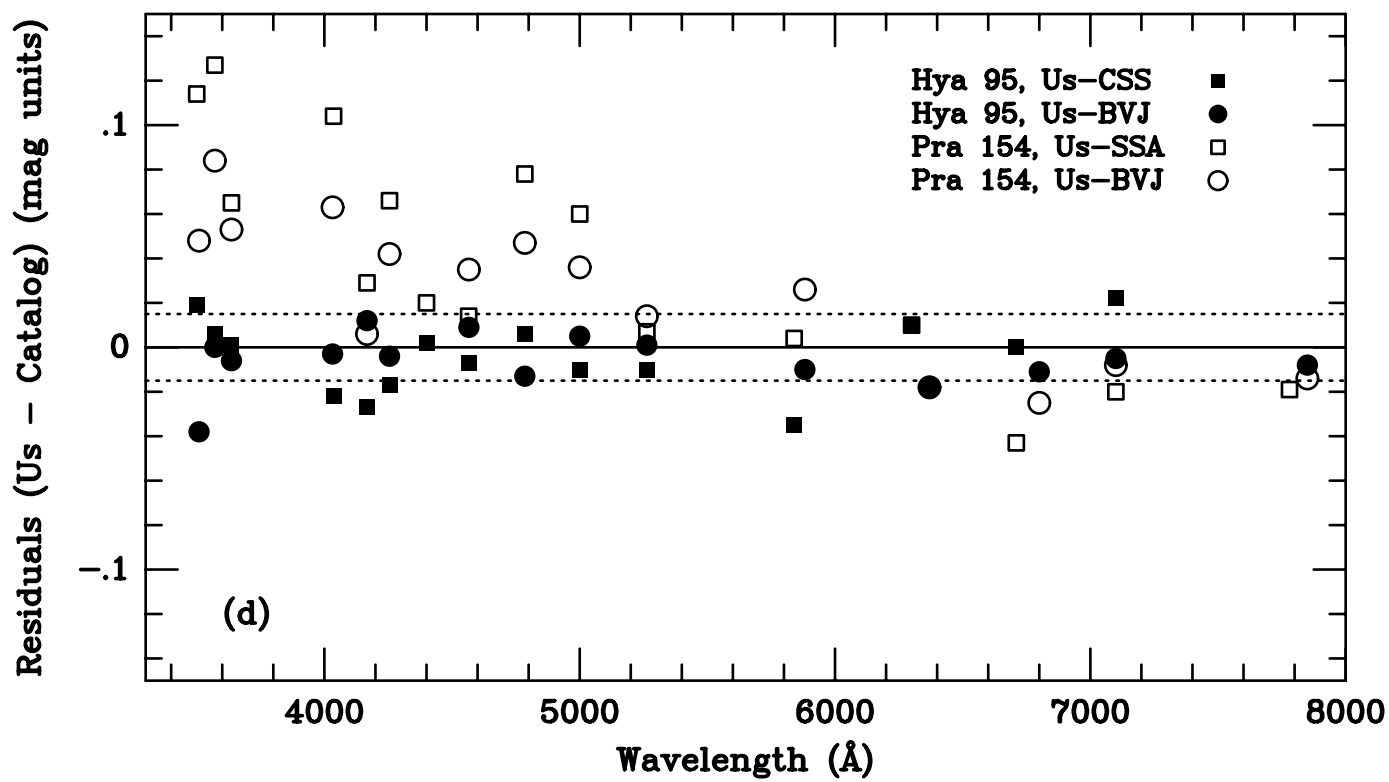
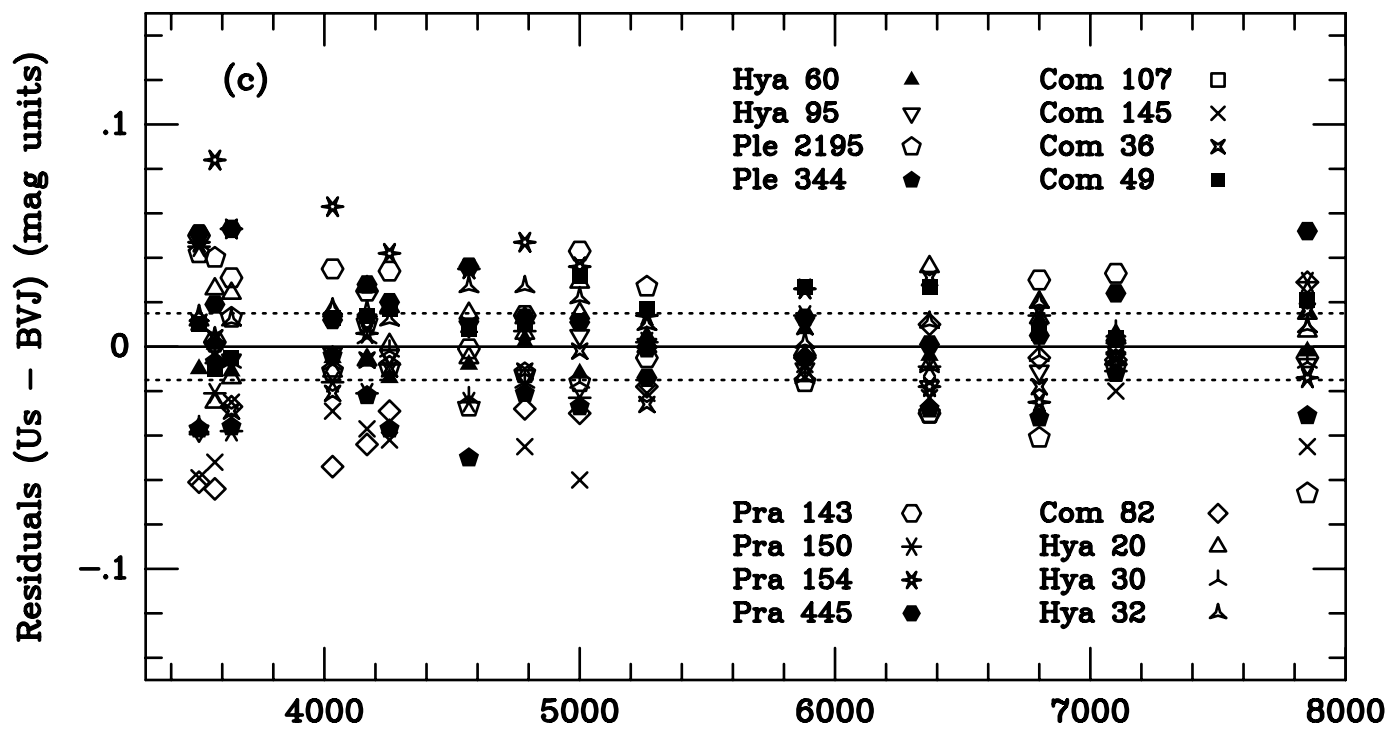
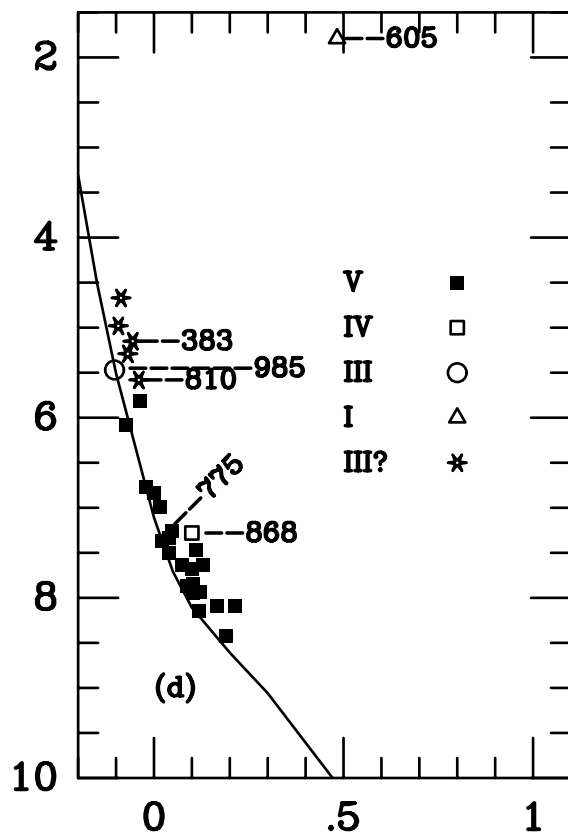
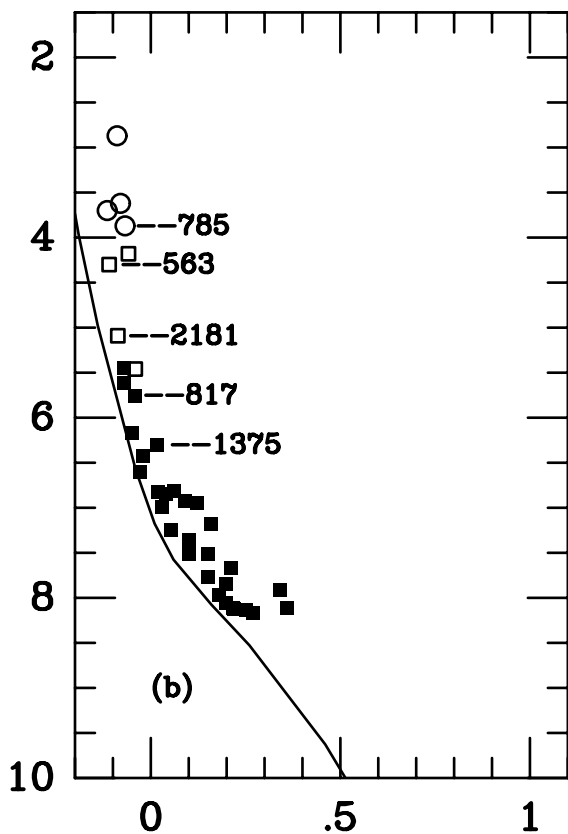
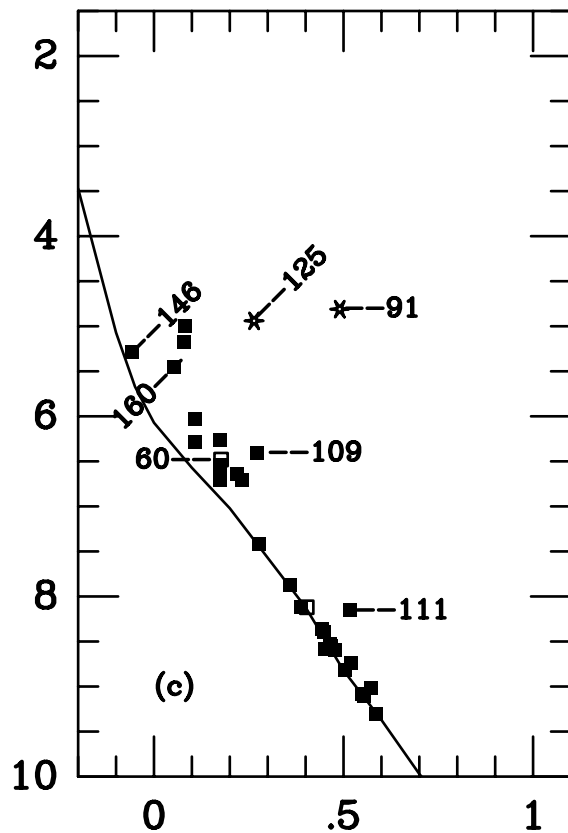
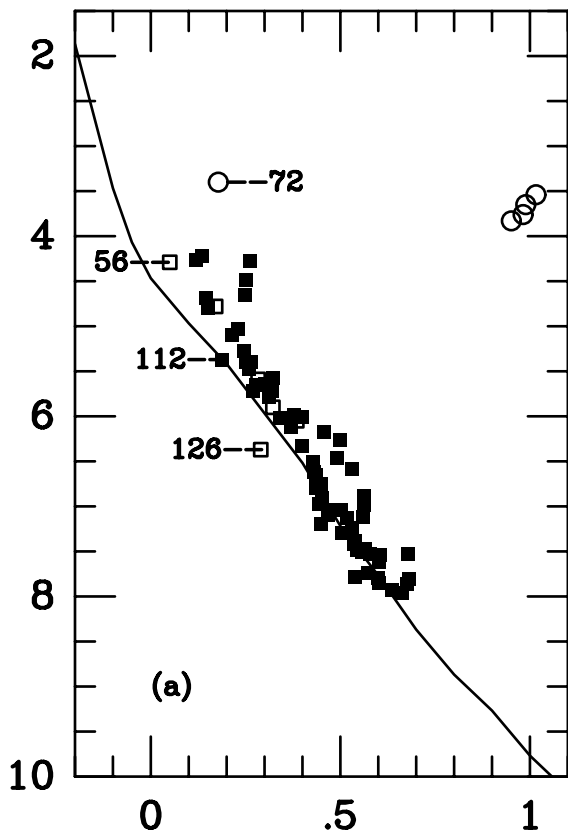
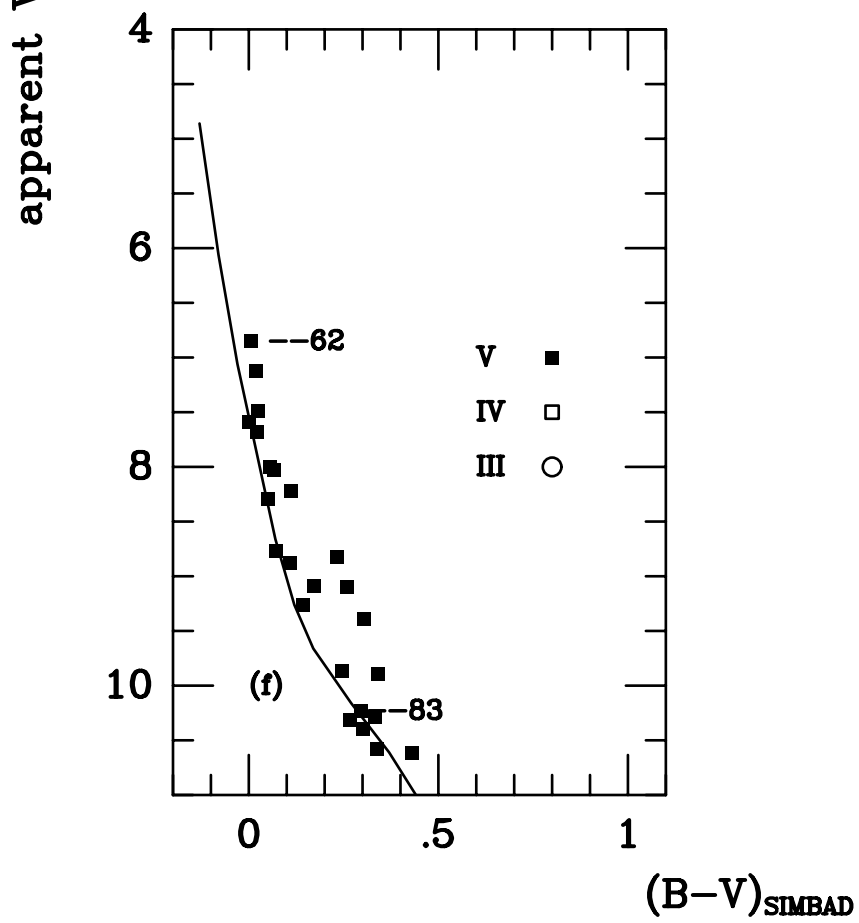
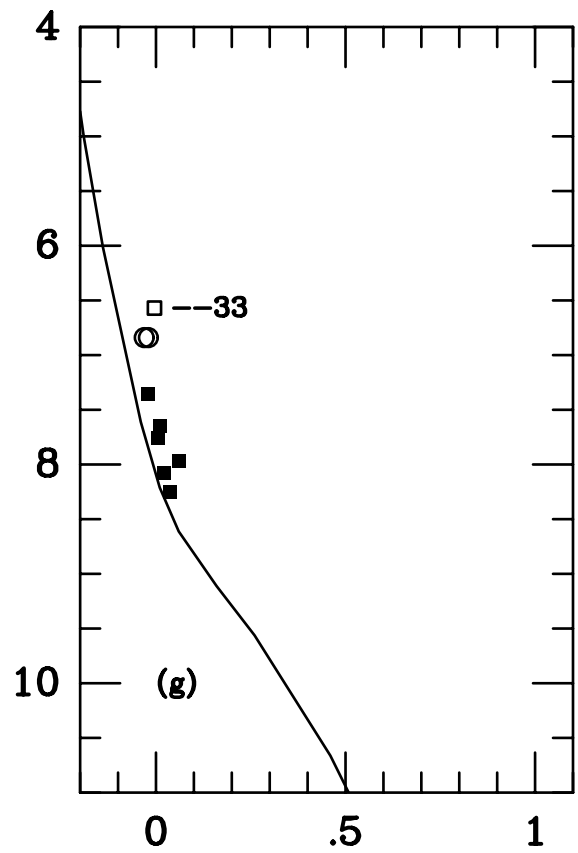
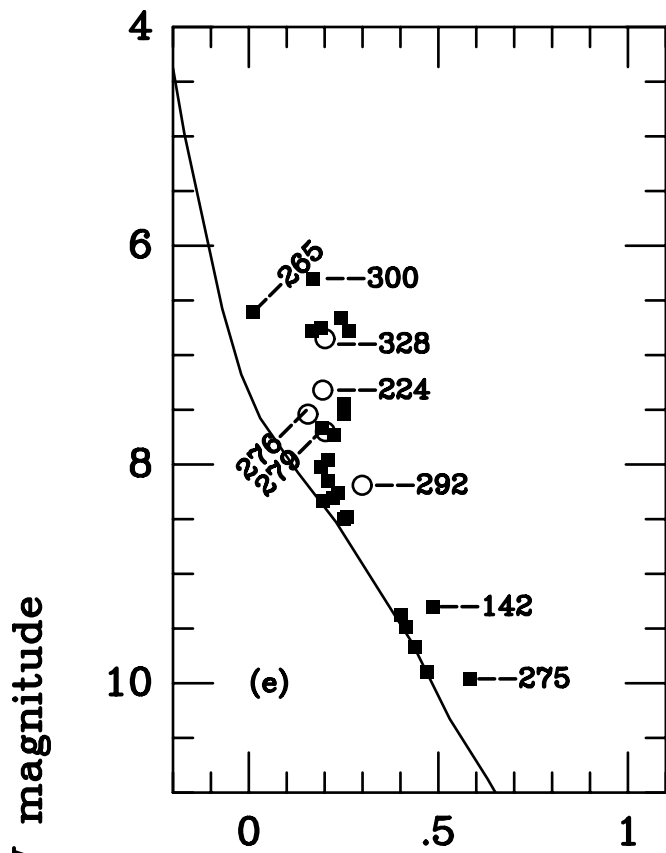


Figure 1c,d  
Clampitt &  
Burstein  
AJ 1997

apparent V magnitude



$(B-V)_{\text{SIMBAD}}$



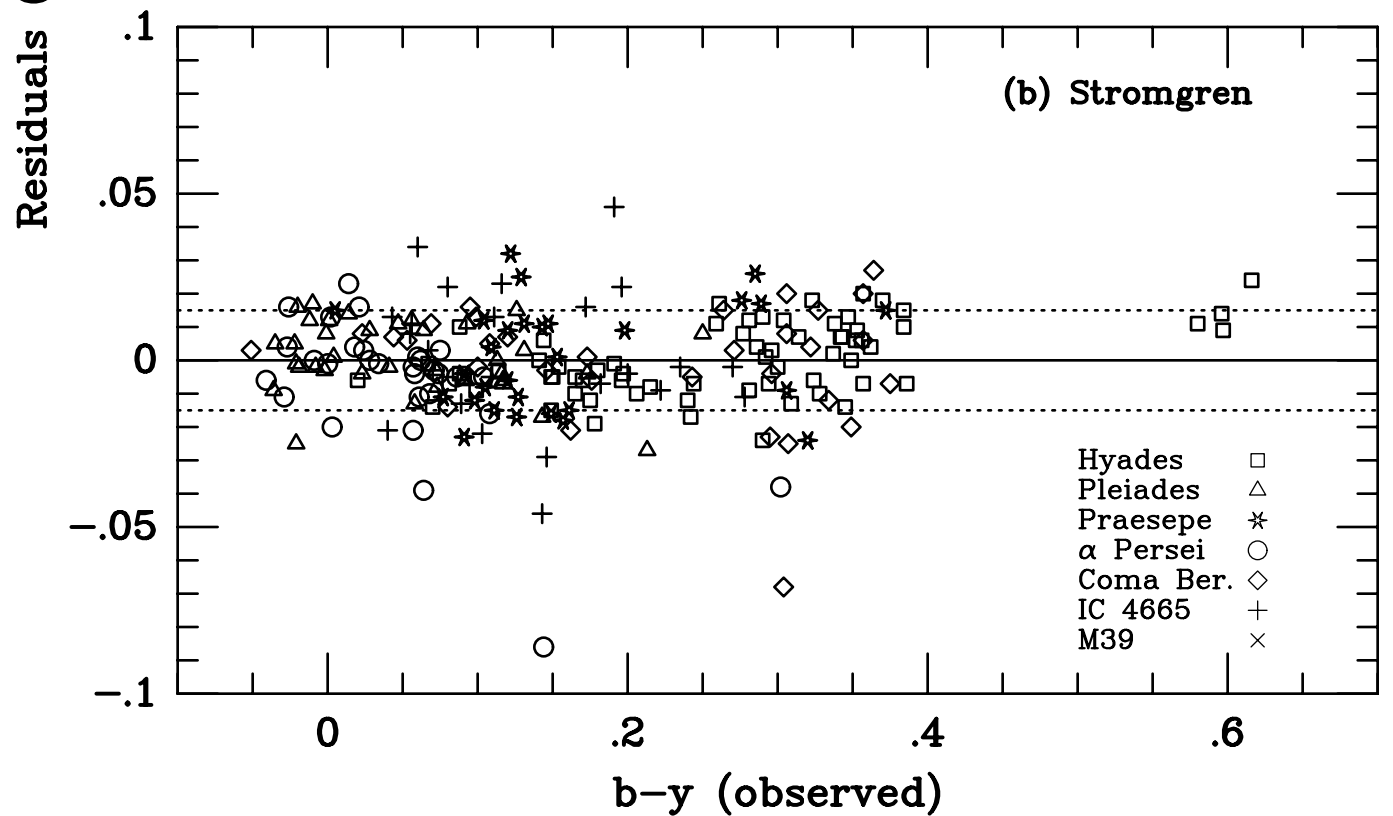
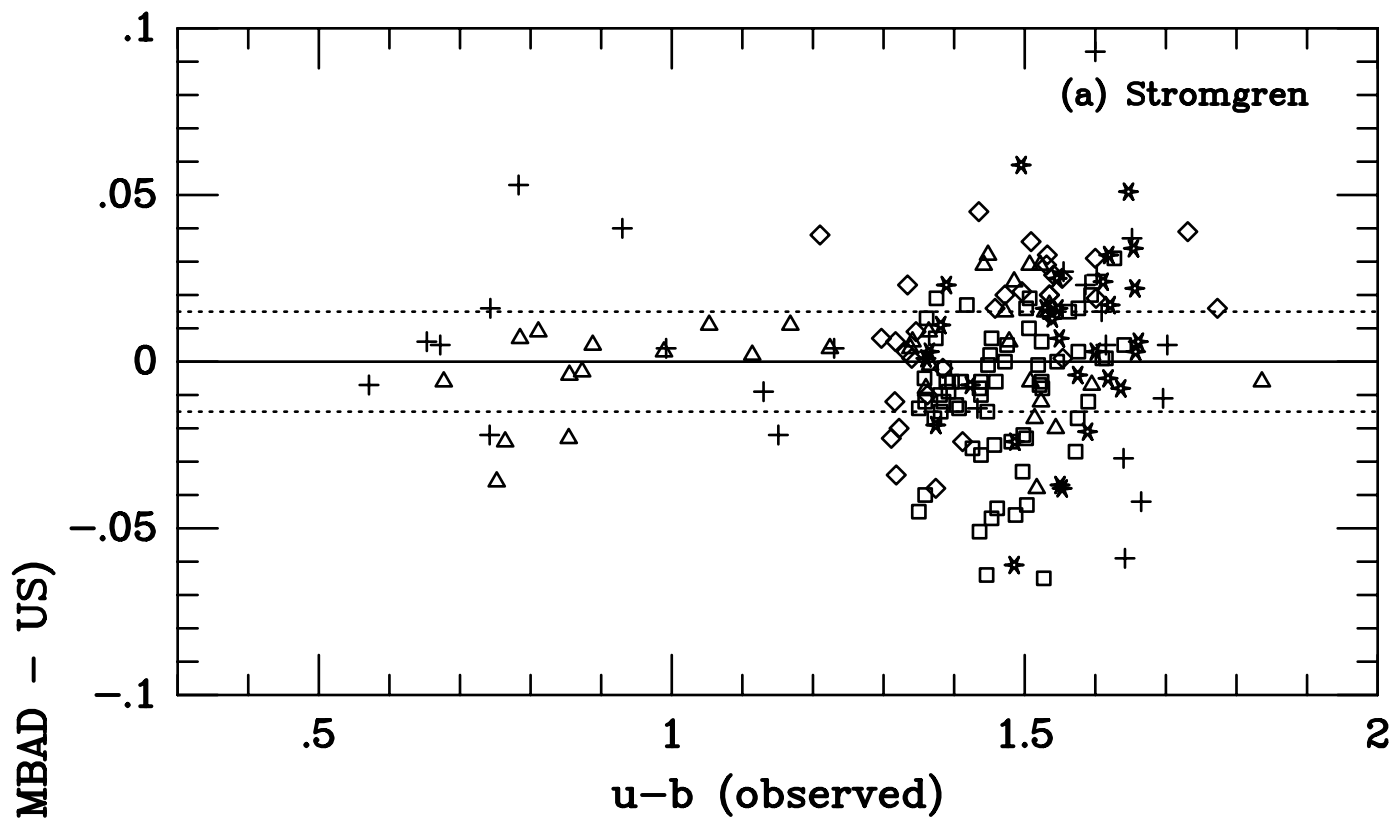
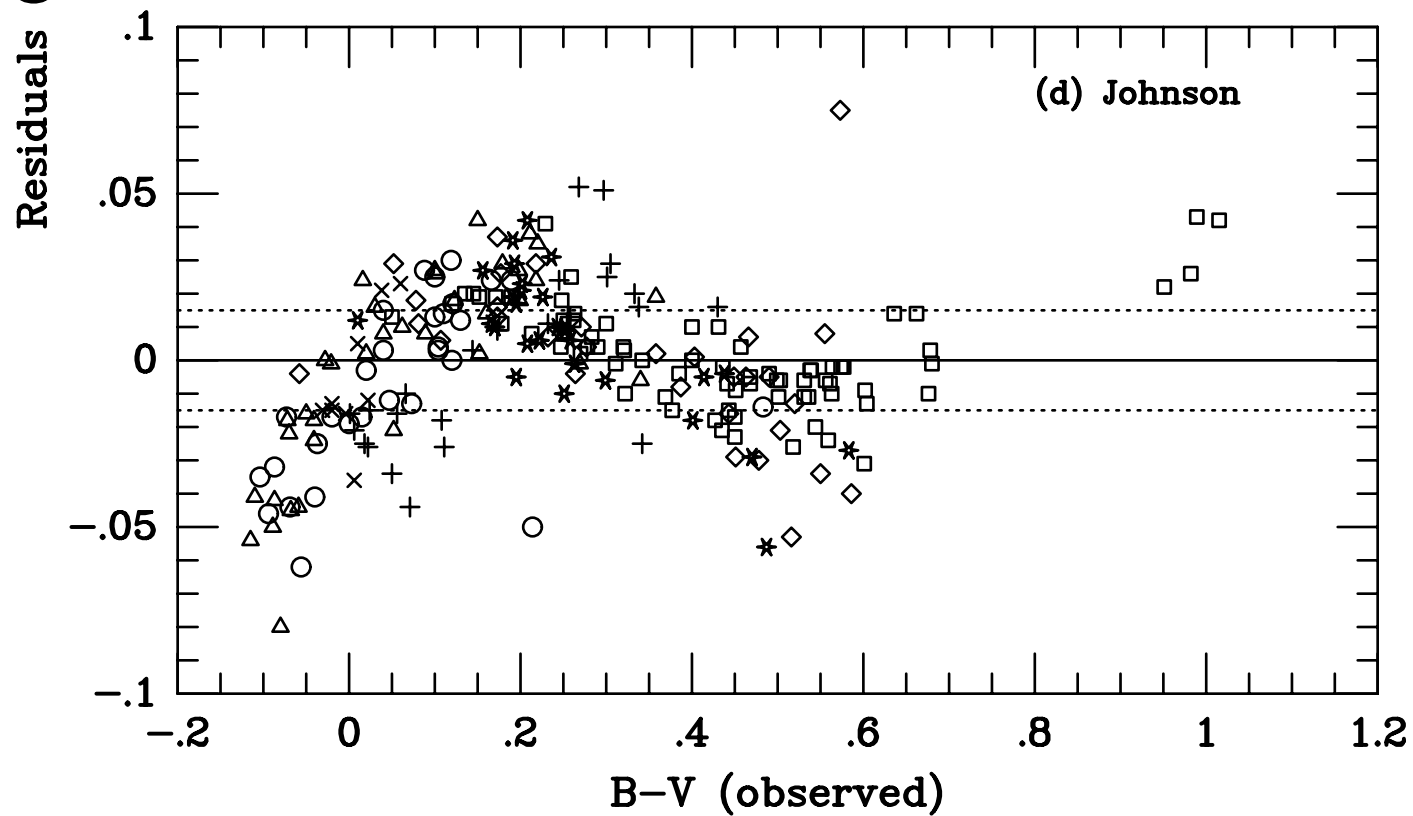
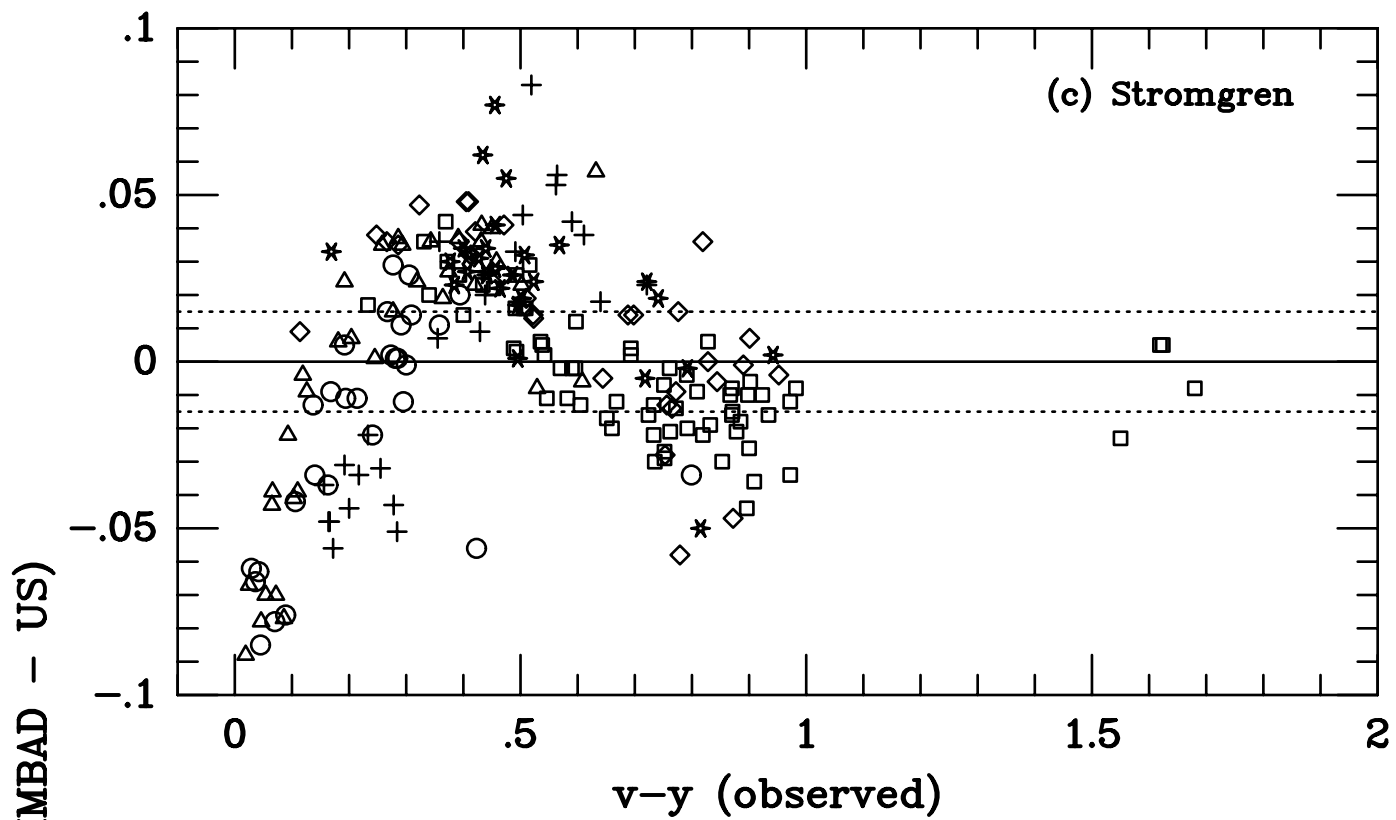


Figure 3a,b  
Clampitt &  
Burstein  
AJ 1997



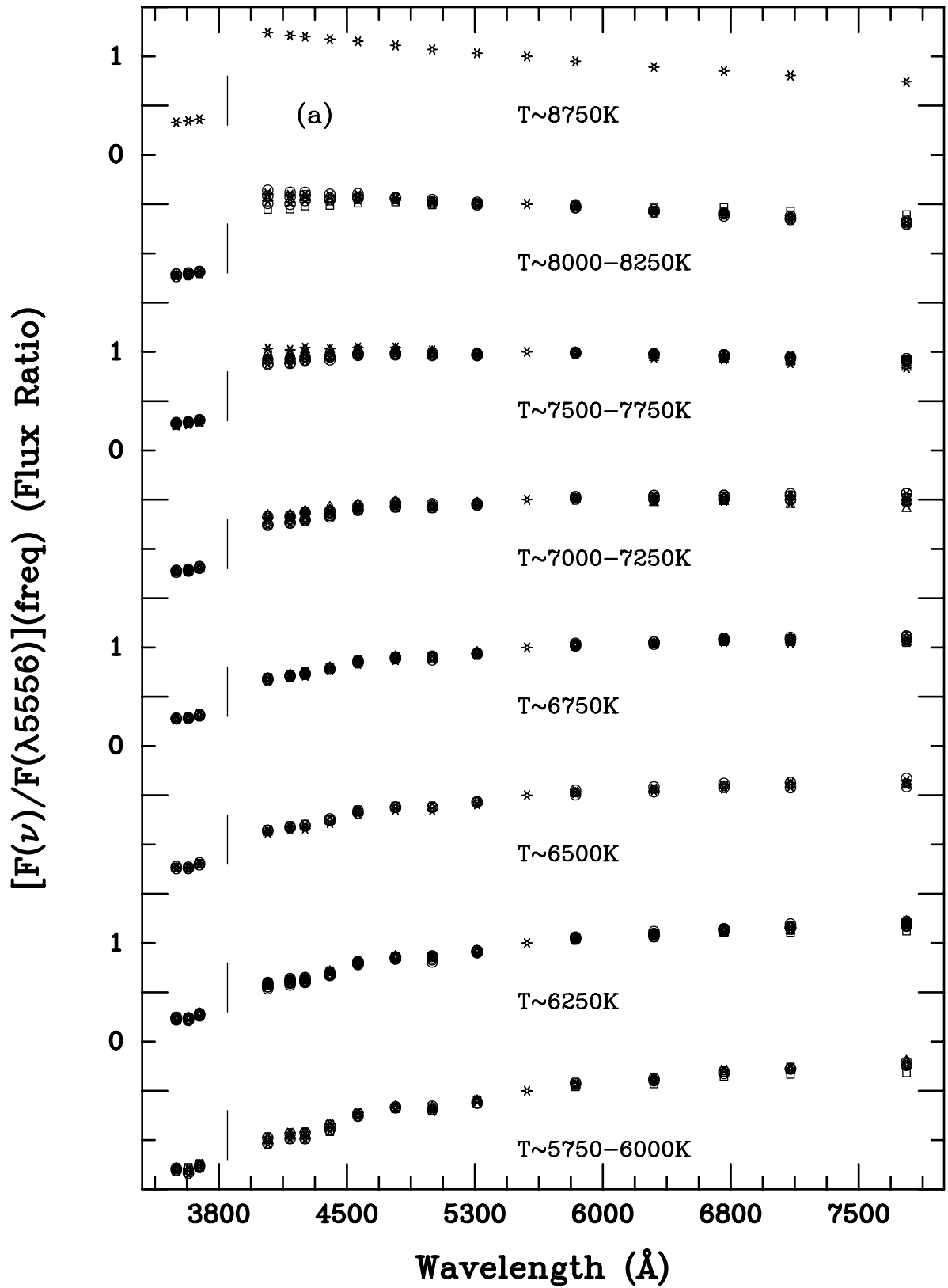


Figure 4a  
 Clampitt &  
 Burstein  
 AJ 1997

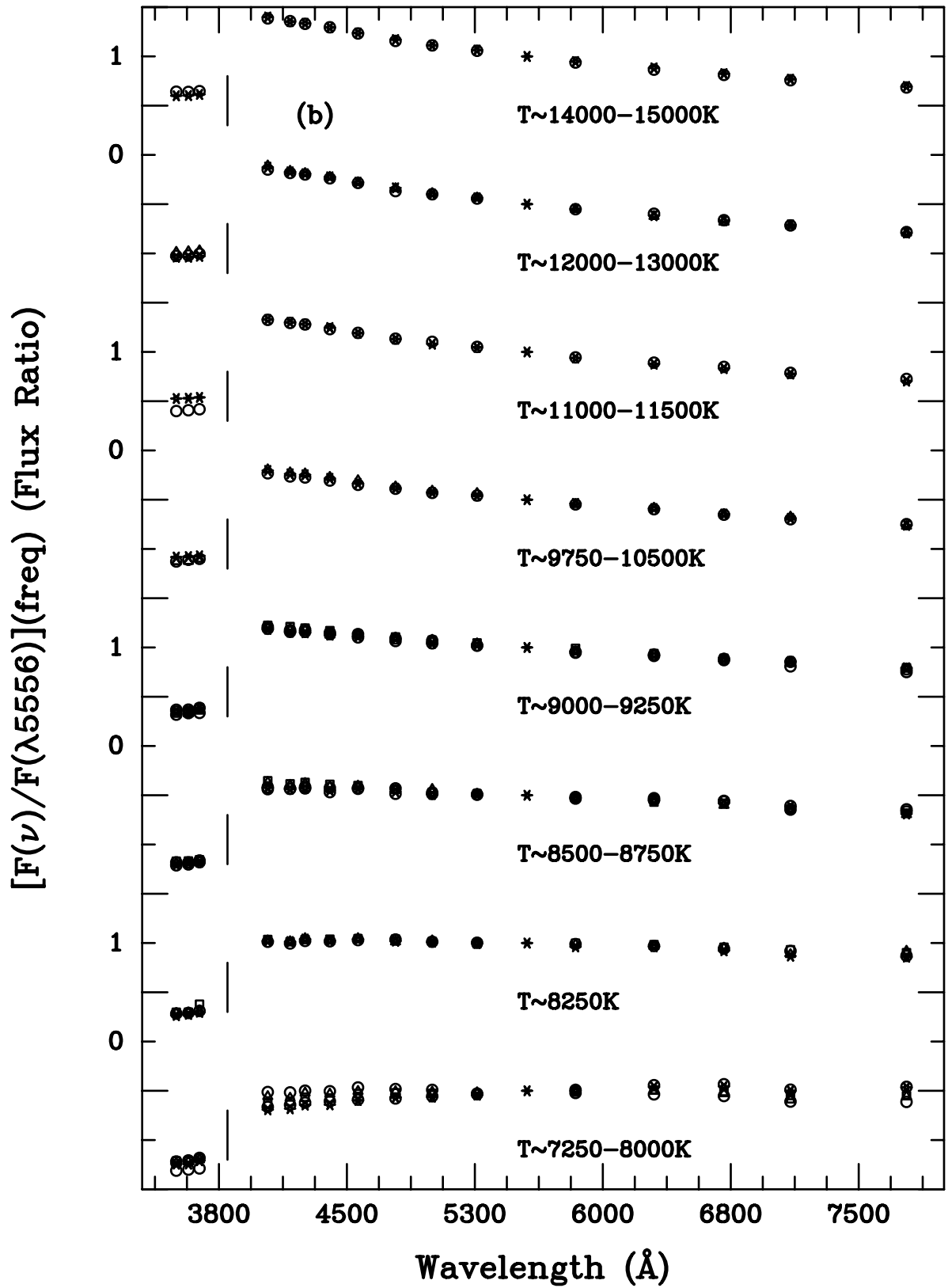


Figure 4b  
 Clampitt &  
 Burstein  
 AJ 1997





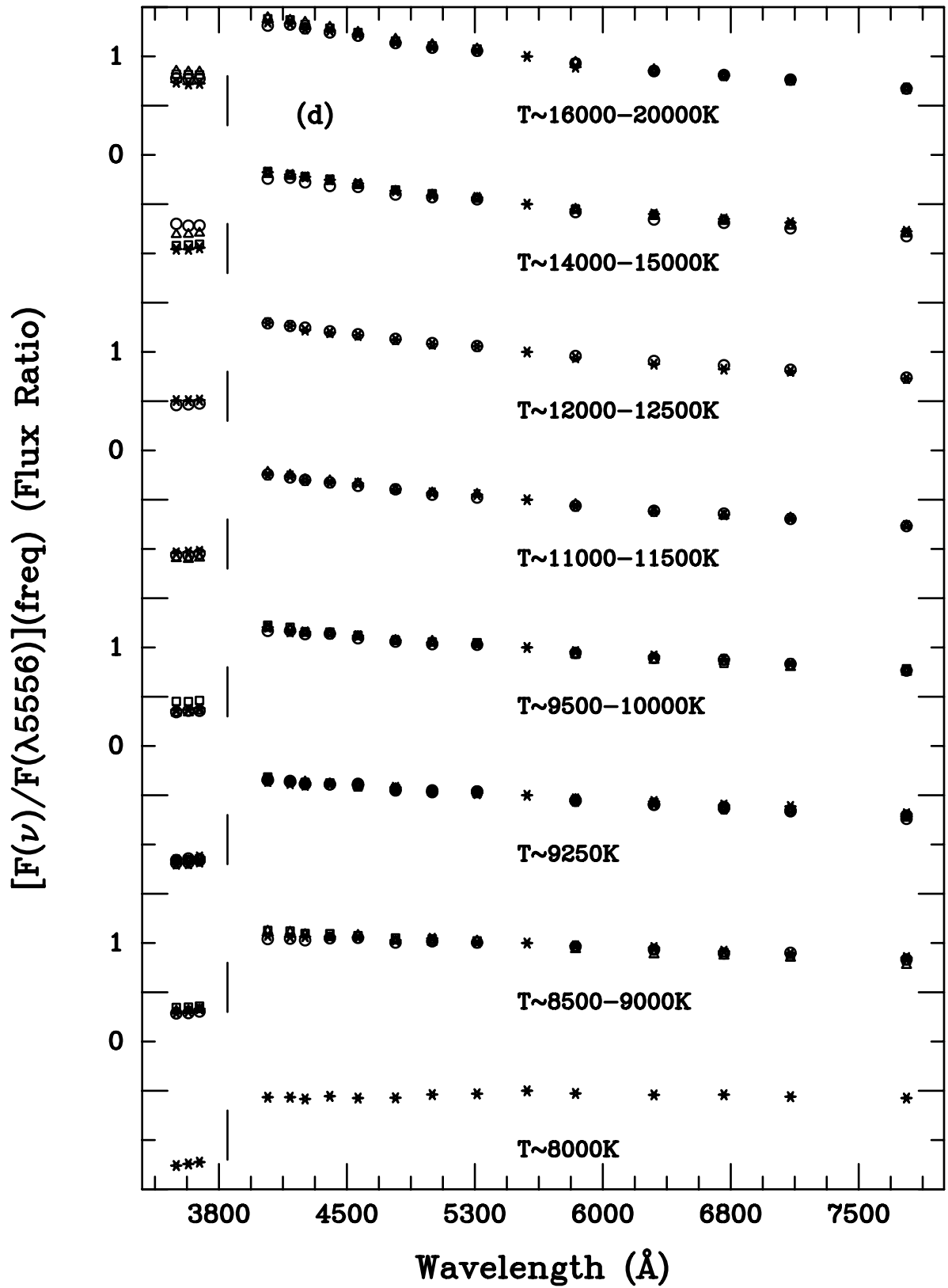


Figure 4d  
 Clampitt &  
 Burstein  
 AJ 1996

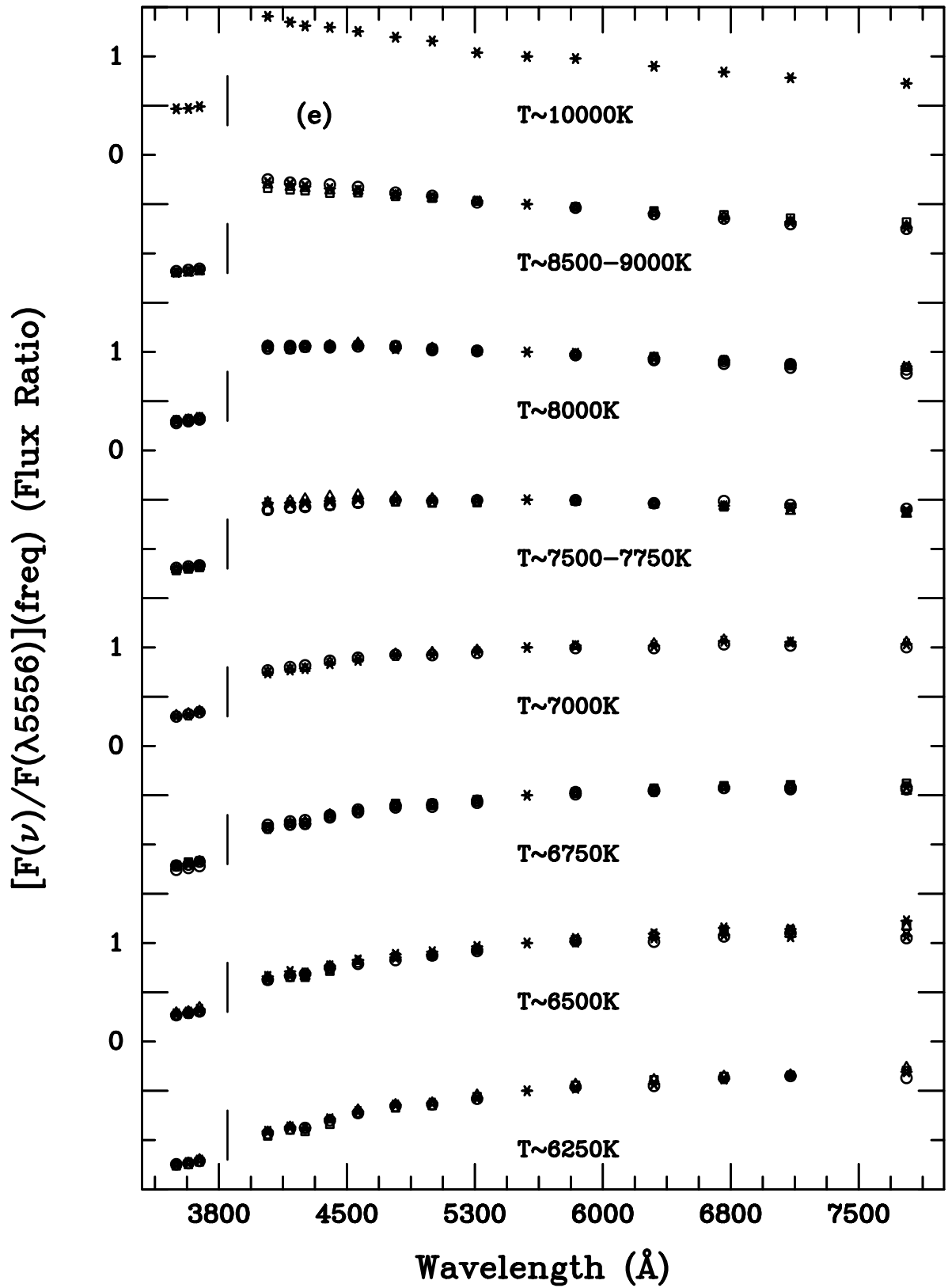


Figure 4e  
 Clampitt &  
 Burstein  
 AJ 1997

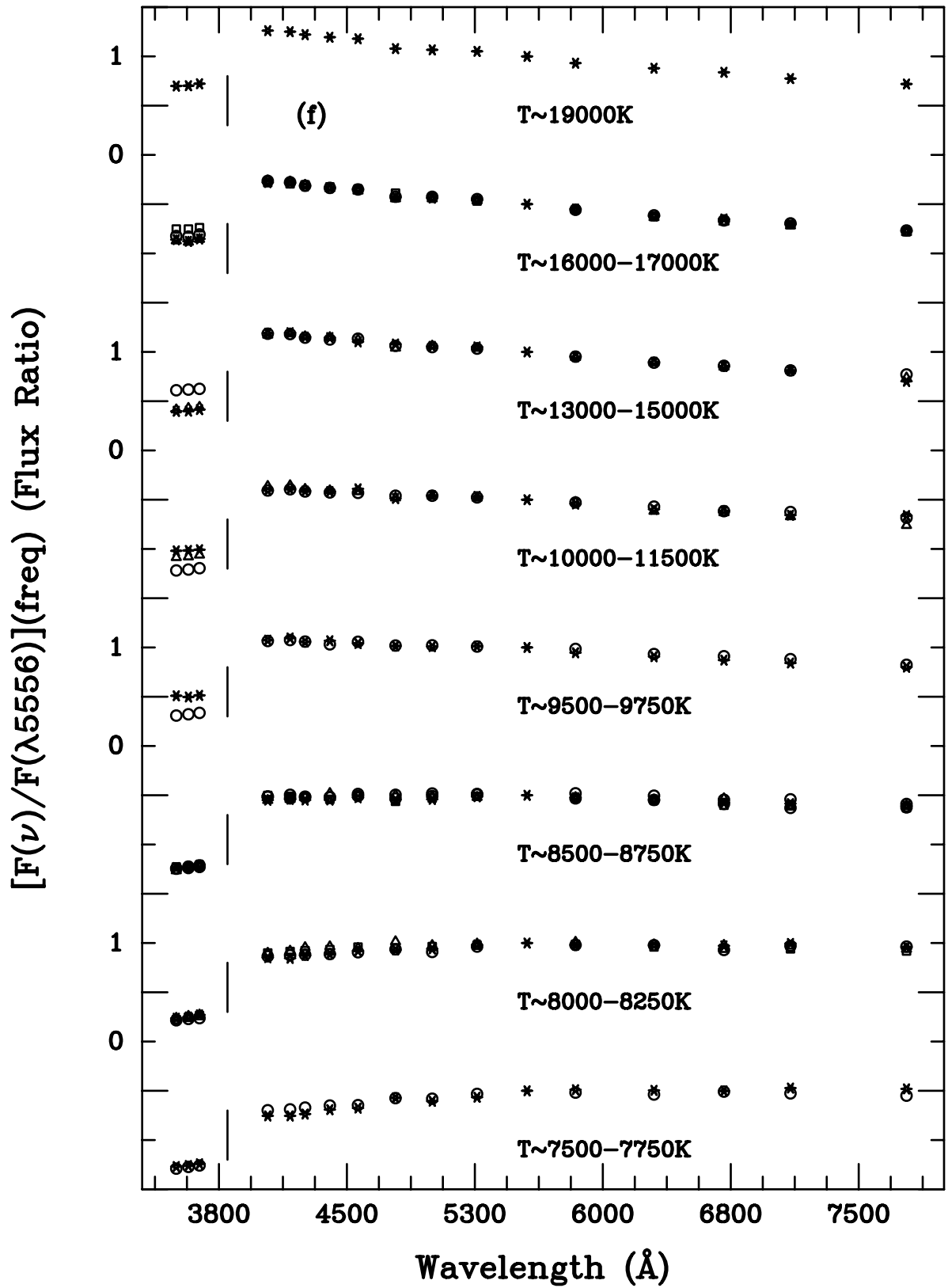


Figure 4f  
 Clampitt &  
 Burstein  
 AJ 1997

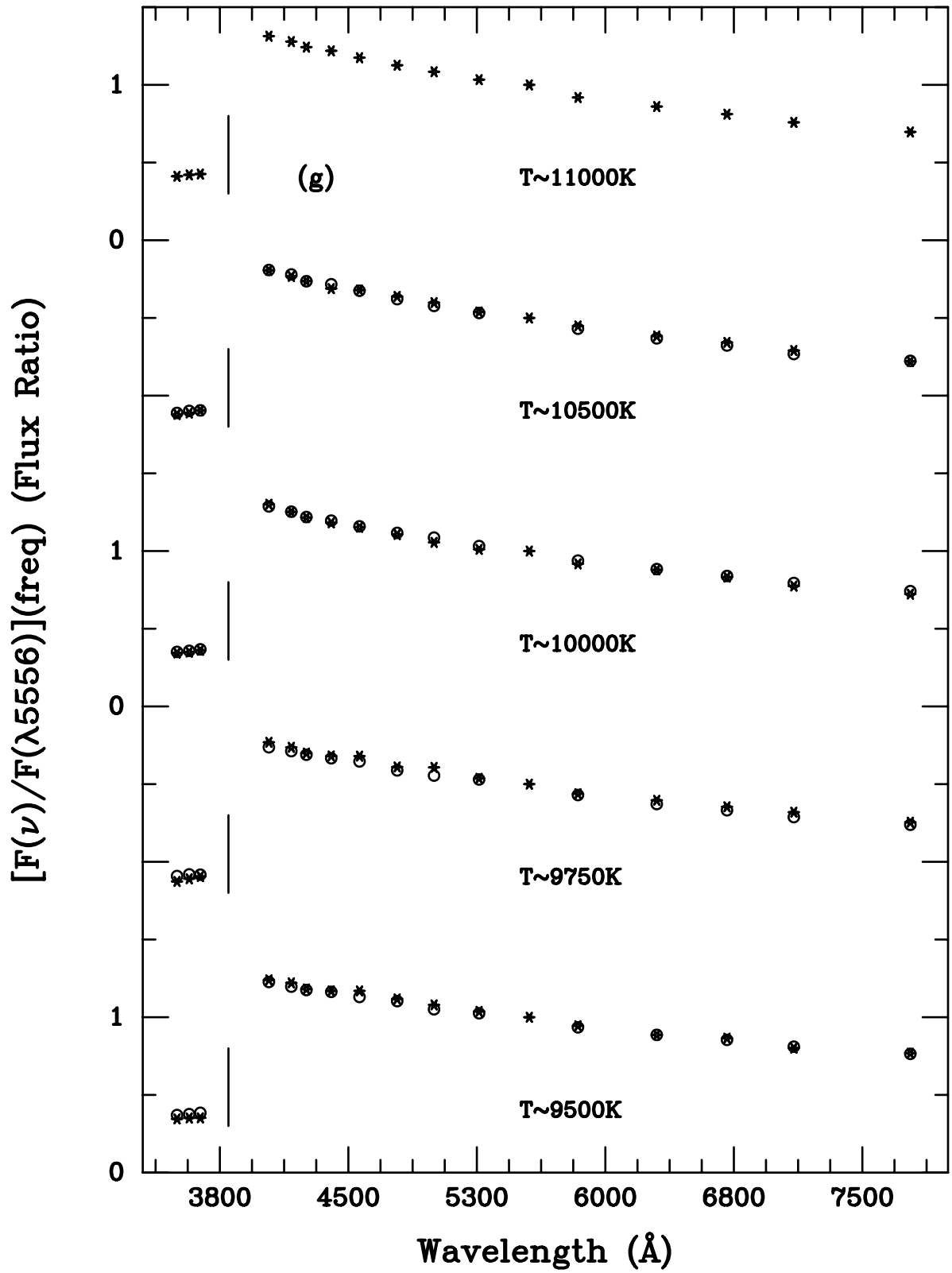


Figure 4g  
 Clampitt &  
 Burstein  
 AJ 1997

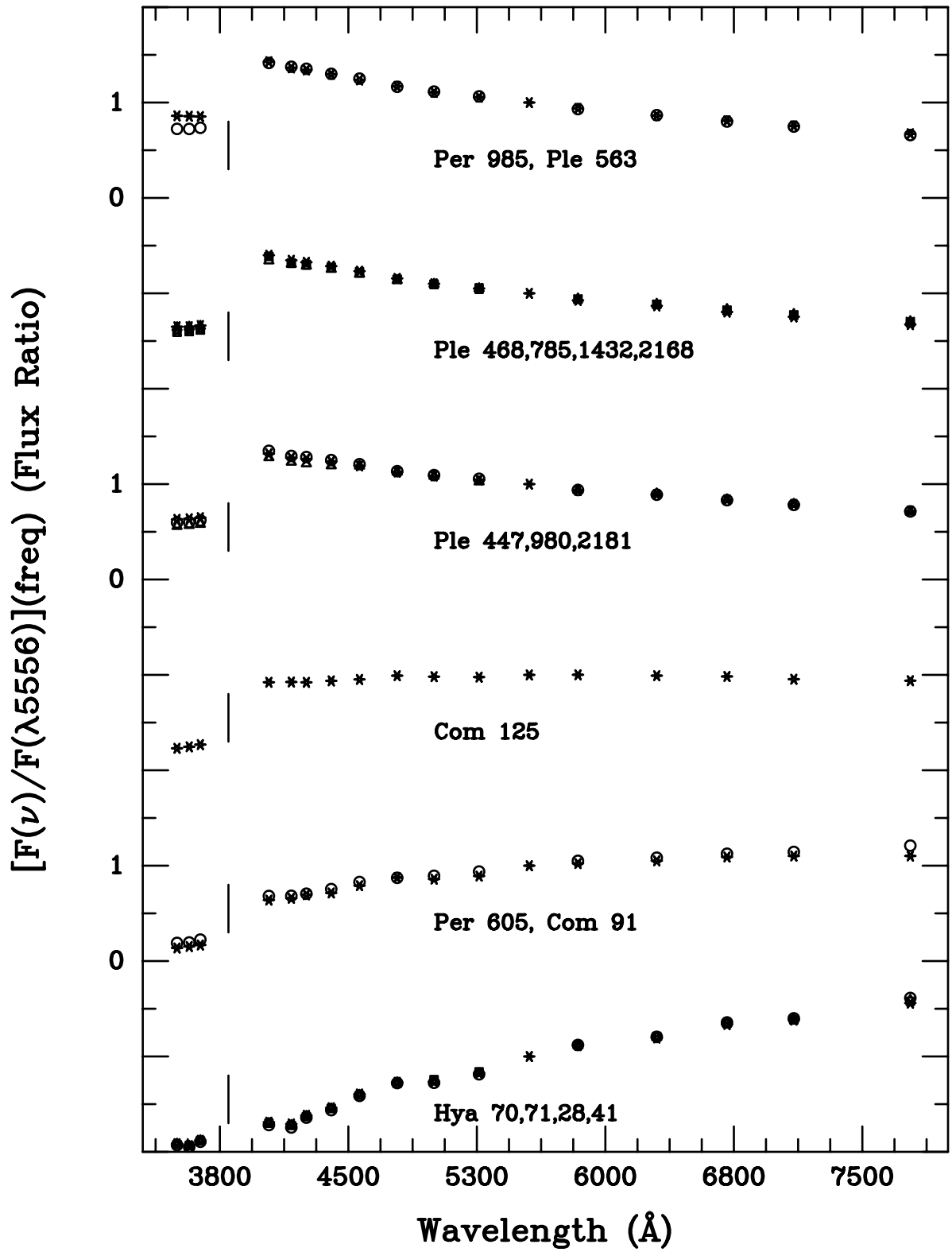
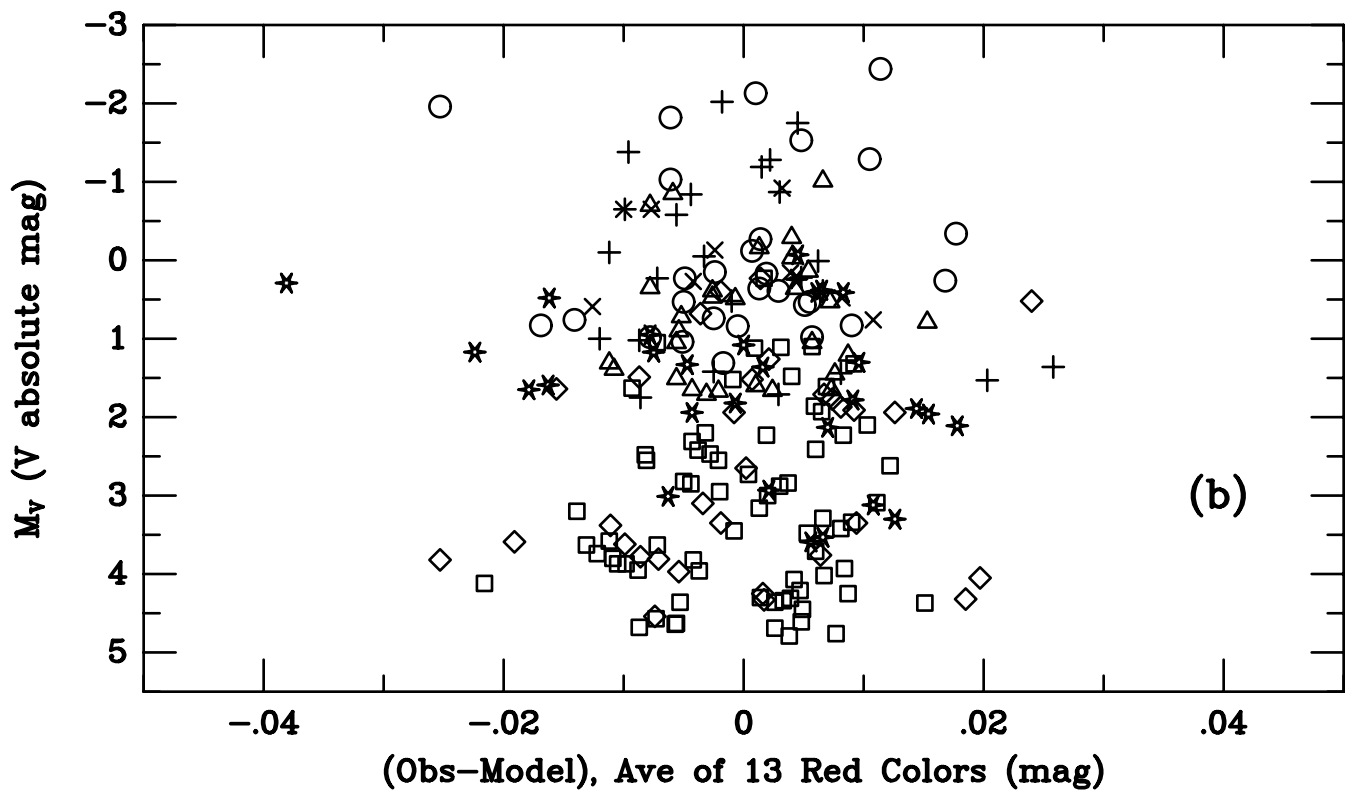
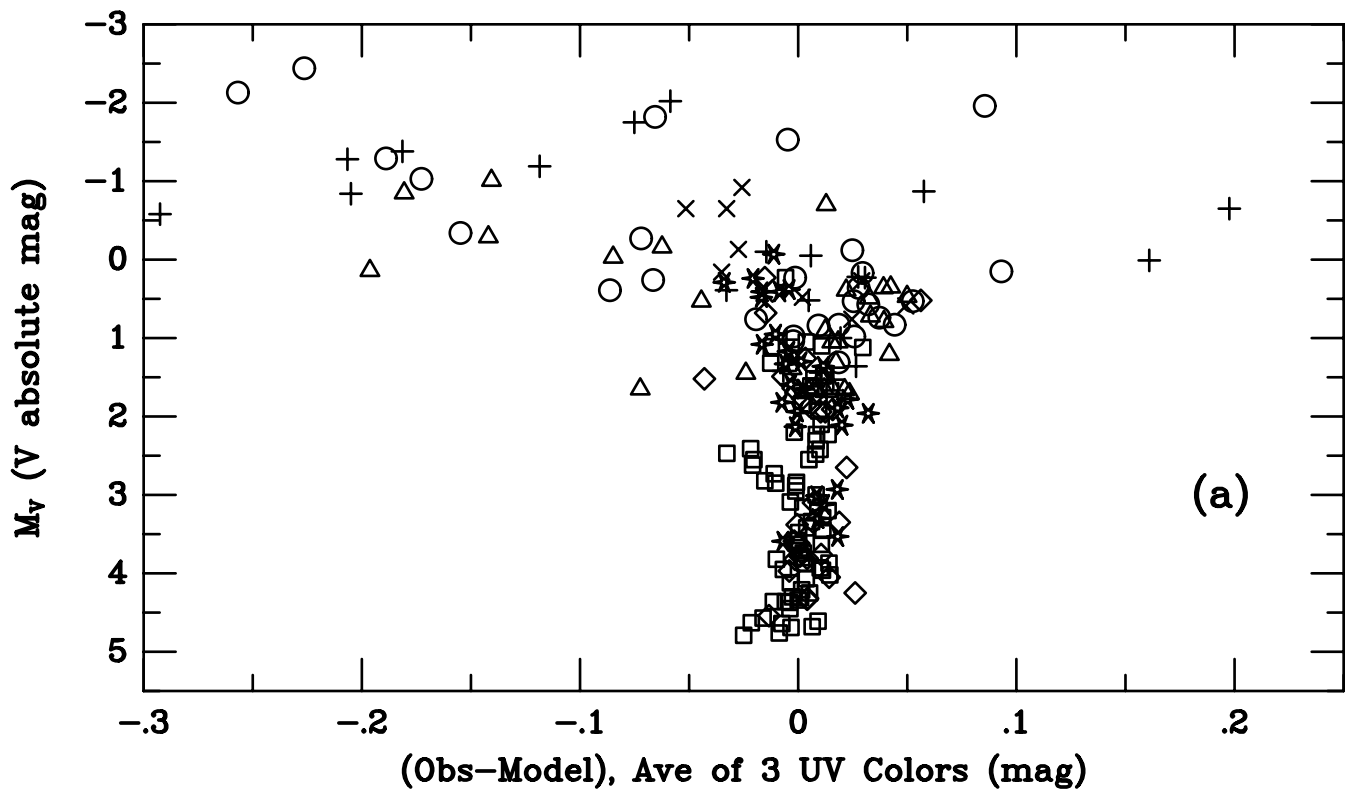


Figure 5  
 Clampitt &  
 Burstein  
 AJ 1997



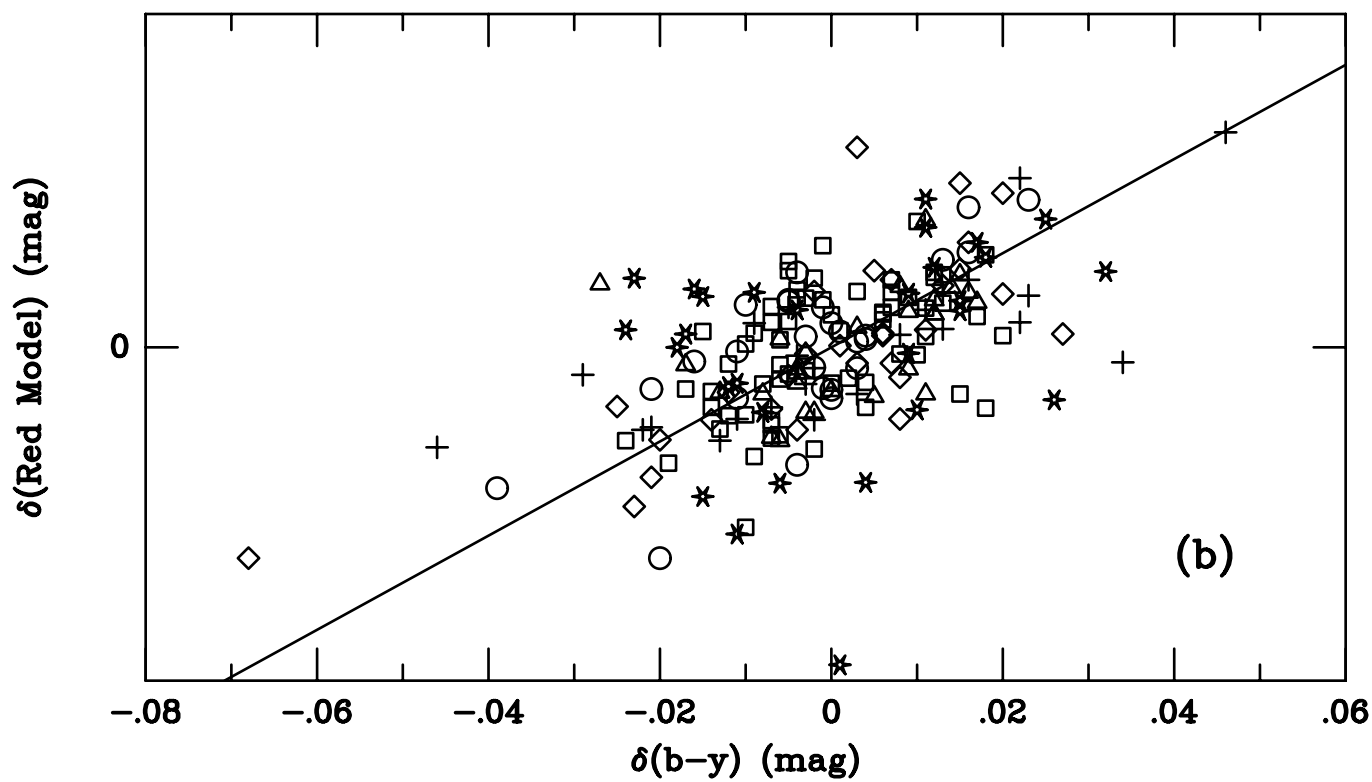
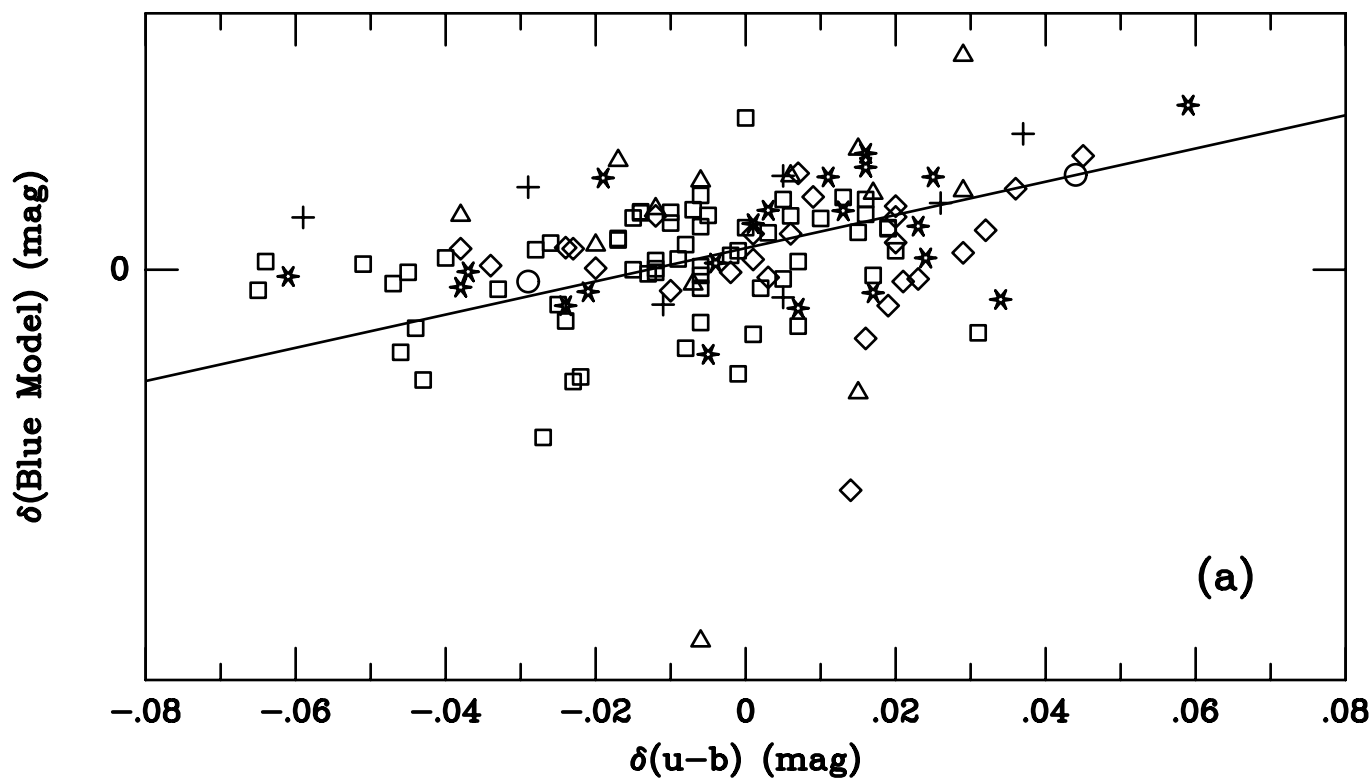


Figure 7a,b  
Clampitt &  
Burstein  
AJ 1997